D3.2 Flight Test Report Phase #1

Julius Bartasevicius (TUM) and Sebastian Köberle (TUM)

GA number: 815058
Project acronym: FLIPASED
Project title: FLIGHT PHASE ADAPTIVE AERO-SERVOELASTIC AIRCRAFT DESIGN METHODS

Funding Scheme: H2020 **ID:** MG-3-1-2018
Latest version of Annex I: 1.1 released on 12/04/2019
Start date of project: 01/09/2019 **Duration:** 40 Months

Lead Beneficiary for this deliverable:	TUM
Author(s): J. Bartasevicius	
Last modified: 31 December 2021	**Status:**
Due date: 30 October 2021	Delivered

Project coordinator name and organisation: Bálint Vanek, SZTAKI
Tel. and email: +36 1 279 6113 vanek@sztaki.hu
Project website: flipased.eu

Dissemination Level:		
CO	Confidential, only for members of the consortium (including the Commission Services)	
PU	Public	X

“This document is part of a project that has received funding from the European Union’s Horizon 2020 research and innovation programme under grant agreement No 815058.”

Glossary

BP	Back-up Pilot
CG	Centre of Gravity
DLR-SR	Institute of System Dynamics and Control (SR), DLR
ECU	Engine Control Unit
EDL	Engineering Data Link
EDMO	Special Airport Oberpfaffenhofen
FBG	Fibre Bragg Grating sensor
FLEXOP	Flutter Free Flight Envelope Expansion for Economical Performance Improvement
FM	Flight Manual
FTC	Flight Test Card
FTE	Flight Test Engineer
FTM	Flight Test Manager
FTO	Flight Test Operator
GCS	Ground Control Station
GPS	Global Positioning System
LiPo	Lithium polymer battery
MAV Link	Micro Air Vehicle Link
ONERA	Office National d'Etudes et de Recherches Aérospatiales (The French Aerospace Lab)
PIC	Pilot-in-Command
RWY	Runway
SZTAKI	Institute for Computer Science and Control
TOW	Take-off Weight
TUD	Technical Univerity of Delft
TUM	Technical University of Munich
UAV	Unmanned aerial vehicle

Table of Contents

1 Executive Summary

One of the main parts of the FLiPASED project is flight testing. This is the method to experimentally evaluate the findings of the project within a real-world environment.

The current document presents the flight test results from phase 1. Phase 1 is the initial phase of the tests, where prerequisites for more complex flutter and load-alleviation testing are checked. Many unforeseen problems were realised in 2020 and 2021. These were: landing gear and ground control issues, bad weather and findings that the aerodynamics of the actual aircraft are not as predicted. None of these challenges were easy to cope with, therefore only two flights were made in phase 1 up to date.

The deliverable describes the taxi testing and the flight tests. Aerodynamic analysis, based on flight test data and simulations, follows. Conclusion and outlook are included at the end of the document.

All the experiments and simulations described in the deliverable were done by TUM.

One note must be made regarding the timing of this deliverable. The date, which was set at the initiation of the project for this deliverable was 31.07.2020. Then, due to taxi problems (described in section 2.3.1), the deliverable was pushed back to 30.10.2021. This deadline was not met due to the following reasons:

- The ground controllability problems were still there during the summer of 2021, as well as problems with the engine. Therefore, up to that date, only one flight was carried out (the second flight was carried out three days before the deadline). It was therefore desired to have more content for the deliverable.
- Additionally, as explained in section 2.4, a flight test campaign as planned for end of September or October. This flight campaign was intended to be sued as the basis for the deliverable. However, the new rules for flight permit application meant that the same persons, who were responsible for the deliverable, had to concentrate on submitting the documents to receive the flight permit. Sadly, the application was not processed in time.
- Furthermore, additional work was required to prepare the aircraft for flights in October. It was therefore decided to prioritise performing the flight tests and using the data for the deliverable.
- Finally, a sub-scale model of the T-FLEX demonstrator has been developed during 2020 (section 3). It was desired to have the results included in this deliverable, as it deals with fundamental understanding of the demonstrator performance.

2 Planning and Execution of Flight Test Phase #1

2.1 Adjusting the Flight Test Plan

After many unsuccessful flight trials in 2020, the flight test plan had to be revisited. Flights for each phase were again redefined. The minimum number of flights according to phases were created (Figure 1) and process chart was made (Figure 2).

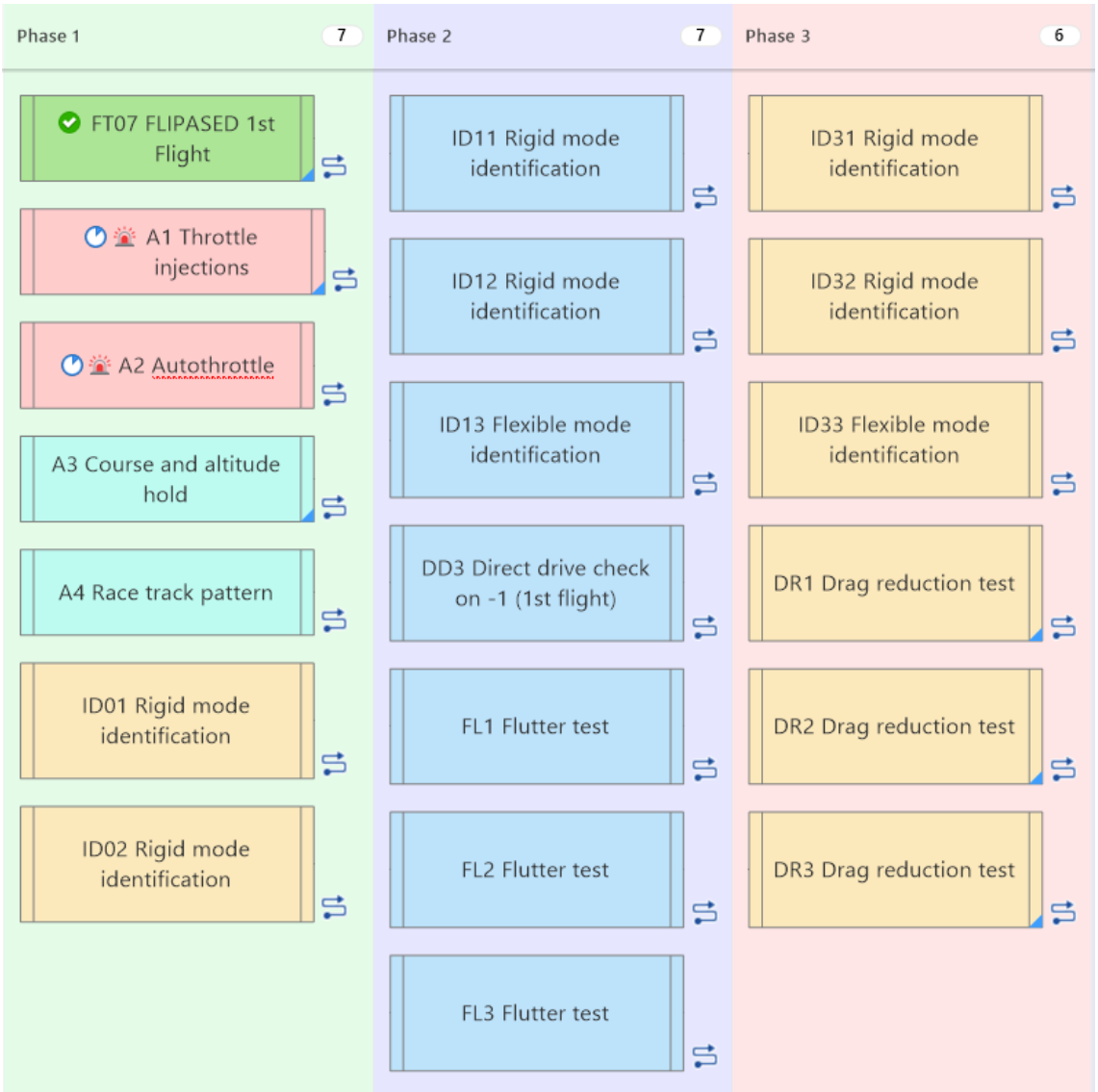

Figure 1 - Flight descriptions split into different phases.

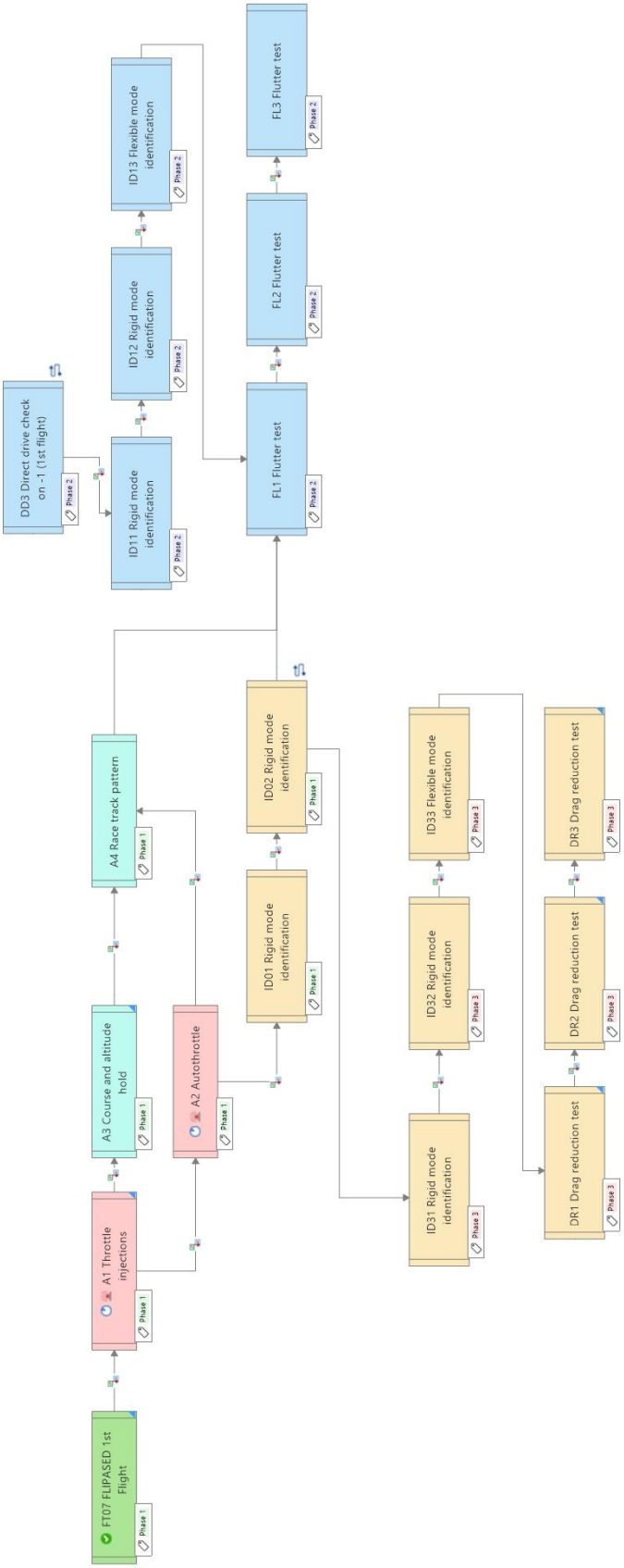

Figure 2 - Redesigned flight test process flowchart.

According to this plan, at least 7 flights were expected for the Flight Test Phase #1. The main topics of the phase remained the same:

1. Testing complete functionality of the autopilot in-flight and
2. Gathering enough data to confirm the rigid flight dynamic and structural dynamic model.

2.2 Summary of Flight-Related Tests

Up-to-date summary of all the tests carried out in relation to the Flight Test Phase #1 was made (Table 1). These include crew training (with the simulator), taxi tests, bigger system checks and actual flight tests or flight test attempts. Note that the flight test only changed the number after a successful flight was made (therefore FT8 is repeated several times). Also, not all the system checks were added to the table.

Table 1 - Summary of testing within Flight Test Phase #1.

#	Name	Date	Problem type	Status	Type	Went to the airfield?
1	Crew Training	29.06.2020		Done	Simulator Training	
2	Taxi Test	23.07.2020		Done	Taxi Test	yes
3	Taxi Test	29.07.2020		Done	Taxi Test	yes
4	Taxi Test	30.07.2020		Done	Taxi Test	yes
5	Taxi Test	22.09.2020	System problem	Aborted	Taxi Test	yes
6	Taxi Test	29.09.2020		Done	Taxi Test	yes
7	Taxi Test	09.10.2020		Done	Taxi Test	yes
8	Taxi Test	15.12.2020		Done	Taxi Test	yes
9	Crew Training	25.02.2021		Done	Simulator Training	
10	Crew Training	20.04.2021		Done	Simulator Training	
11	FT7	21.04.2021		Done	Flight Test	yes
12	Crew Training	29.04.2021		Done	Simulator Training	
13	FT8	11.05.2021	System problem	Aborted	Flight Test	yes
14	Crew Training	26.05.2021		Done	Simulator Training	
15	FT8	15.06.2021	System problem	Aborted	Flight Test	yes
16	FT8	06.07.2021	System problem	Aborted	Flight Test	yes
17	Full system check	19.07.2021		Done	System Test	
18	Engine testing	03.08.2021	System problem	Done	System Test	
19	Engine Testing	03.09.2021	System problem	Done	System Test	
20	FT8	22.09.2021	System problem	Aborted	Flight Test	yes
21	Taxi Test	20.10.2021		Done	Taxi Test	yes
22	FT8	27.10.2021		Done	Flight Test	yes
23	FT9	21.11.2021		Done	Flight Test	yes

Within the last 16 months, 8 taxi test days were made, 5 crew training sessions and 7 flight attempts (3 were successful). The crew went to the airfield on 15 days. Out of these times, the required tests could not be completed on 5 occasions due to various reasons.

2.3 Taxi tests

The initial year of the project was busy solving the landing gear issues. These issues have already been described in the 1st Periodic Report but are also added here for completeness.

2.3.1 Description of taxi testing in 2020

The project for TUM has started with a demonstrator, which has already been used in the previous project, FLEXOP. The demonstrator has performed six flight tests up to then. However, building on previous experience, landing gear proved to be one of the biggest challenges during the operation of the demonstrator. The aircraft was very difficult to control while on the ground, leading to a few very dangerous situations and one accident, where the aircraft skidded of the runway and hit a runway light. Therefore, upgrades were necesary to ensure sustainable operation of the aircraft.

Figure 3 - T-FLEX Demonstrator during the last flight within the FLEXOP project.

As a starting point, the following design flaws have been identified:

1. The maximum angle of attack, achieved on the ground, is limited by very low main landing gear and a high tail wheel. This design solution limits the maximum angle of attack that could be achieved for takeoff to 3.3deg. This is very small for a taildragger aircraft and usually would be around 10deg. In addition, fixing such a design on an already manufactured aircraft is not easy.
2. Very narrow main landing gear makes it easy for the aircraft to bank from wingtip to wingtip. If this happens during takeoff or landing, the wingtip touches the ground and instantly creates a destabilizing moment.
3. Main landing gear is longitudinally far from the center of gravity. This means that the disturbing bank angle, required to tip the aircraft, is further decreased.
4. The tires of the main landing gear are too soft for the airplane. This makes it possible to deform the tires very easily and significantly increases the rolling resistance during take-off run.
5. Unsteerable tail wheel makes the aircraft very hard to control while on the ground. The tail must be lifted up first and aircraft is then steered with the rudder.
6. Retractable main landing gear proved to be an unnecessary design add-on to the aircraft which adds complexity, but not value to the demonstrator overall.

These problems were hard to identify during the conceptual or preliminary design phase of the FLEXOP project and were only realized during operations. Therefore, further discussion was held how to make the controllability of the aircraft better.

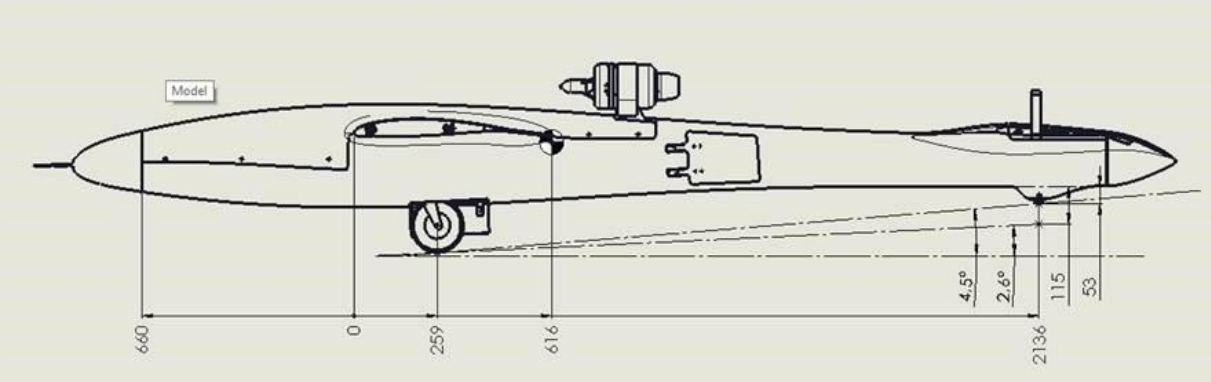

Figure 4 - Comparison of the maximum angle of attack during take-off. 4.5 degrees is the initial tailstrike angle, 2.6 degrees is the tailstrike angle with steerable tailwheel assembly (wing incidence angle is -1.2 degrees).

Two different concepts for fixing the landing gear were discussed:

1. Fundamentally changing the landing gear layout.
2. Adjusting the current landing gear to make it acceptably safe for operation.

Because the first option would require major fuselage changes and would take at least a few months, it was decided to start with the second option first. Ways to improve handling were discussed during the winter before the first flight test campaign. Due to the complex nature of the problem the solutions that were initially agreed upon did not completely resolve the issue. This resulted in an iterative process with different concepts being implemented as add-ons to the initial design along the way. The chronology of the process was:

1. Implement the steerable tailwheel with damping
    a. The initial solution to steering was to install an off-the-shelf tailwheel assembly. Unfortunately, the solution did not work because the load on the tailwheel appeared to be too big for the part. Therefore another, completely custom iteration was done. This included a custom milled aluminum fork for steering and a damping assembly. The damping assembly was composed of glass-fiber-reinforced plastic plate acting as a leaf spring for longitudinal damping and two rubber dampers for lateral stiffness. The structure held well, but the steering made the aircraft hard to control and very sensitive to any pilot inputs.
2. Change the brakes of the main landing gear to more effective ones
    a. Tire brakes were changed to drum brakes. From previous testing it was noted that the tires wear out very quickly due to the brakes. Also, the braking power of the old system proved to be too little. Therefore, new type of brakes was implemented that would both conserve the tires and increase the braking force on the wheel hub.
3. Add a gyro to the tailwheel
    a. Introducing the steerable tailwheel did not solve the controlability problem as the team has hoped. The aircraft became very sensitive, especially at higher speeds. The solution was to introduce a gyroscope-based compensation for the gain on the steering. This proved to improve the steering somewhat.
4. Reverse the main landing gear frame to shift the ground contact point back
    a. One of the main findings, mentioned in the early research on taildragger aircraft is that the tendency to veer of the runway is decreased if the centre of gravity is kept as close as possible to the main landing gear. This was recorded in all the reports on the topic.

Therefore, changing the location of the landing gear was considered. Luckily, the landing gear frame was easy to flip, moving the main landing gear backwards by 75mm. The outcome was lesser tendency to veer off the runway, an increase to the critical bank angle to tip on one wing, but also higher load on the main tires. Even though the weight increase was only 2.5% per wheel, the main tires were already overloaded before. The further steps would include looking for stiffer main tires, if possible.

5. Laterally stiffen the main landing gear assembly
    a. During the taxi tests cameras were mounted facing both the gears. This helped to observe the behavior of the landing gear and make further conclusions. One of them was that the main landing gear is too flexible laterally, which makes it easier to tip onto one wing and harder to get out of the tipped position. Therefore, further parts were introduced to stiffen the landing gear laterally.
6. Change the main wheels to stiffer ones
    a. Even though the gear was made stiffer, it was recognized that the tyres of the main gear are way too soft for the aircraft. This was discovered during one of the testing days, where the aircraft stood on the ground for a couple of hours. As a result, the foam-filled tyres deformed plastically and were not usable anymore. Additionally, during high-speed taxi tests a set of tyres burst into pieces after they got too hot (Due to braking and rolling). It was decided that a stiffer tyre is a must. And with no alternative tyres available for the same wheelset, a double sailplane tailwheel (TOST 150 MINI) instead of the original RC model grade wheels were bought. The TOST wheels would have a proper inflatable tyre moutned on, which would make the main gear stiffer laterally.
7. Add brakes with higher efficiency
    a. In addition to upgrading the wheels to stiffer ones, the TOST wheels also had a possibility to have disc brakes mounted on them. Since long braking path was also discovered to be a problem during our flight tests, this seemed like a good option.

The changes of both, main gear and tailwheel resulted in a considerably more steerable aircraft. Multiple taxi tests were done, including low speed and high-speed tests, to make sure the aircraft has enough controllability to safely resume flight testing. In the end, changing the main wheels from RC model grade to aviation grade seemed to make the biggest difference. The aircraft was declared as flight-worthy again.

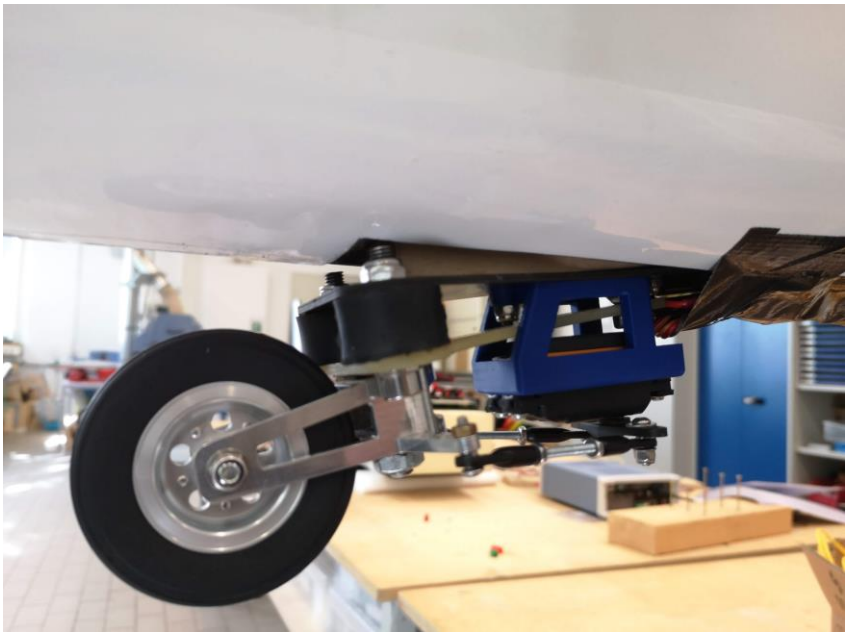

Figure 5 - Steerable tailwheel assembly.

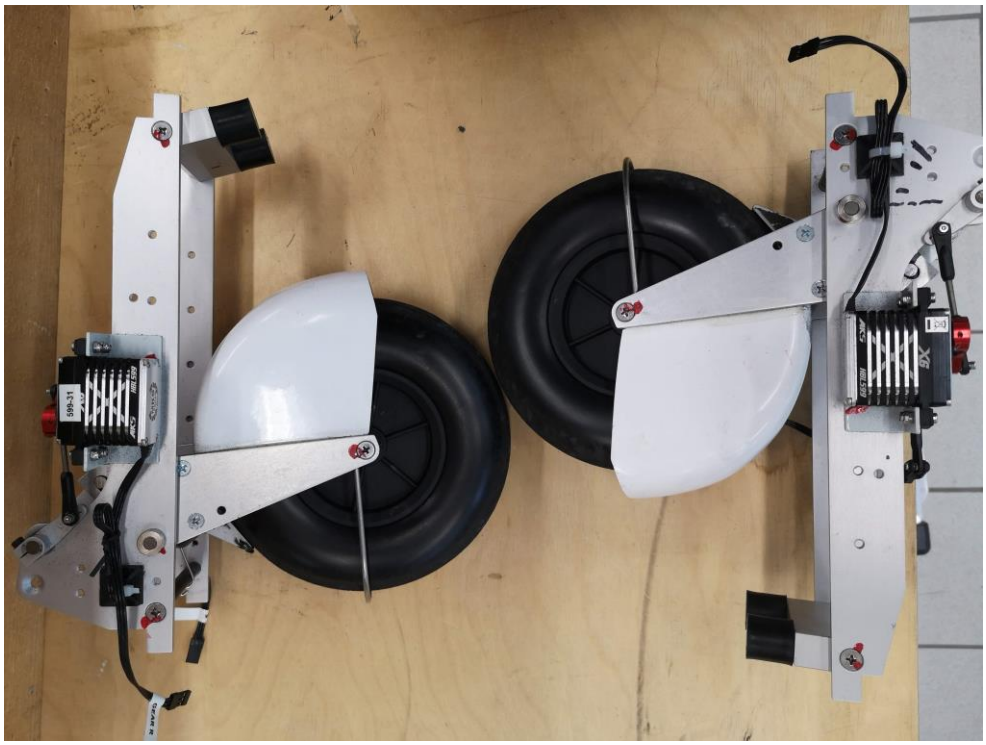

Figure 6 - Comparison of two possible positions for the main landing gear. The difference is around 75mm.

Figure 7 - Too soft tires deforming under normal load.

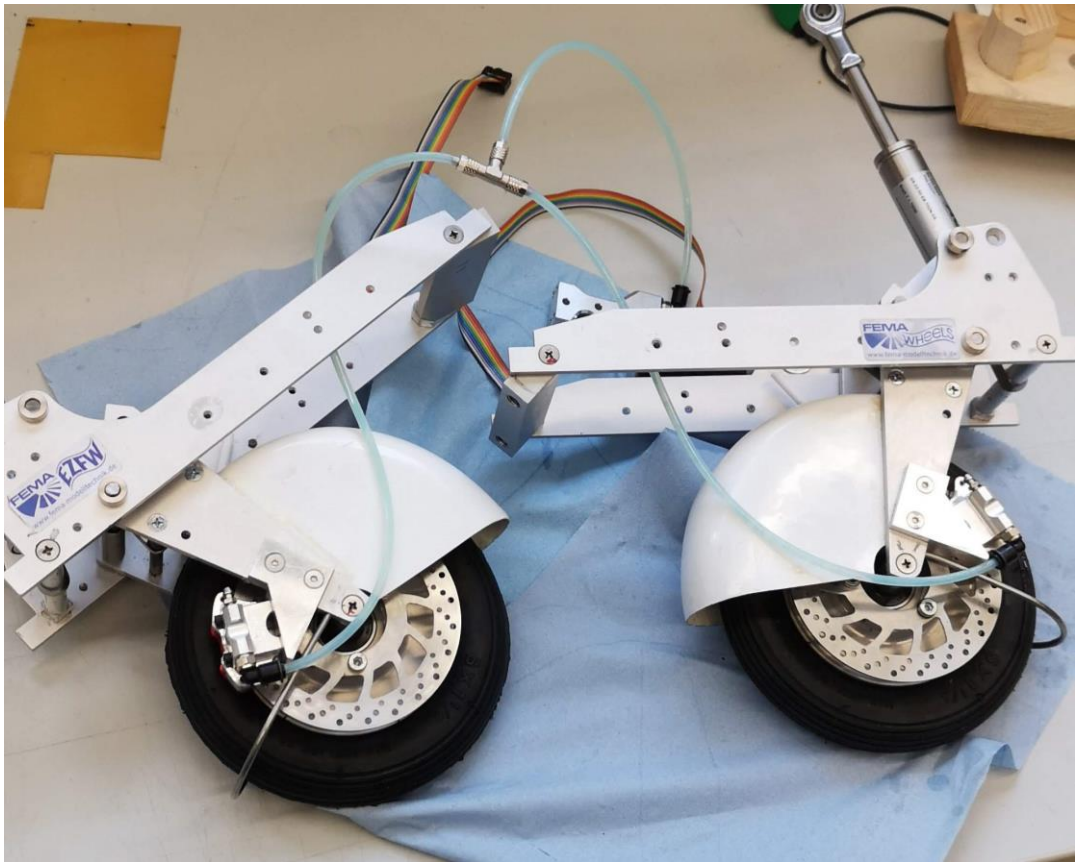

Figure 8 - New main wheels being fitted with disc brakes before instalation.

2.4 Application for flight permit for 2022

In January 2021 the rules for flight permits for UAVs in Germany have changed.

The organization which handles the permits changed from the Bavarian to the National Aviation Authority of Germany (LBA). This increases the processing times of applications.

Moreover, and more importantly, the UAV flight safety rules which were applied to T-FLEX at the beginning of FLEXOP project in 2018 have now changed significantly. The flight permit is only issued if the risk assessment process (SORA), provided by the EASA (https://www.easa.europa.eu/document-library/easy-access-rules/online-publications/easy-access-rules-unmanned-aircraft-systems?page=4%23%5FToc18667479), is followed. These rules not only are more detailed than before, but they are also stricter.

During the summer it was decided to perform a flight test campaign at Cochstedt UAV Flight Test Centre (which belongs to the DLR) end of September or beginning of October. The application process for a flight permit was started mid-August. At that moment the LBA announced that it could take around 6 weeks to process it.

It was soon realized the big amount of work needed to submit the application. The new rules meant that flight areas had to be recalculated, further simulations (for the parachute) be done, manuals updated. Risk analysis had to be rewritten. The final application (100 pages long) was finally submitted on 30.09.2021, after having multiple feedback talks with the LBA. The first reply with request for further corrections of application was received on 26.10.2021. It meant that the flight campaign for this year had to be cancelled.

Now the process is still ongoing. The flight permit is likely to be accepted for Cochstedt airport for 2022. However, as this is not in near viscinity of Munich, where the flight crew is based, organization of flight tests might become more difficult.

Process for a flight permit for Oberpfaffenhofen is not yet started and will be initiated in December.

3 Testing of the DeFStaR Subscale Demonstrator

During the FLEXOP project, discussion of aerodynamic characteristics of the demonstrator was held. It was suggested that the demonstrator might have a dangerous pitch-up stall behaviour. It was decided to investigate the dangerous effect with a scaled version of the T-FLEX demonstrator.

In the following chapter, the motivation and efforts for designing, building and testing dynamic demonstrator for testing the stall behaviour of the *T-FLEX* research aircraft is described. If not marked otherwise, the figures, results and evaluations were created by the student Bastian Scheufele during a research internship titled ***De****monstrator for* ***F****LEXOP* ***Sta****ll* ***R****ecovery* and Master's thesis titled *Development, Flight-Testing and Evaluation of a Subscale Dynamic Demonstrator to Reproduce the Stall Behavior of a Large Swept Wing Research UAV* [1]. The following chapter is an excerpt of the research done in the aforementioned theses describing the motivation and considerations, the resulting subscale demonstrator and flight test results.

3.1 Motivation and Design Goals

Swept wings are known to have dangerous stall characteristics. In such configurations, stall begins at the wing-tips and could lead to a shift of neutral point to the front of the center of gravity. Consequently, this leads to an aerodynamically unstable configuration. This process is exemplified in the following Figure 9.

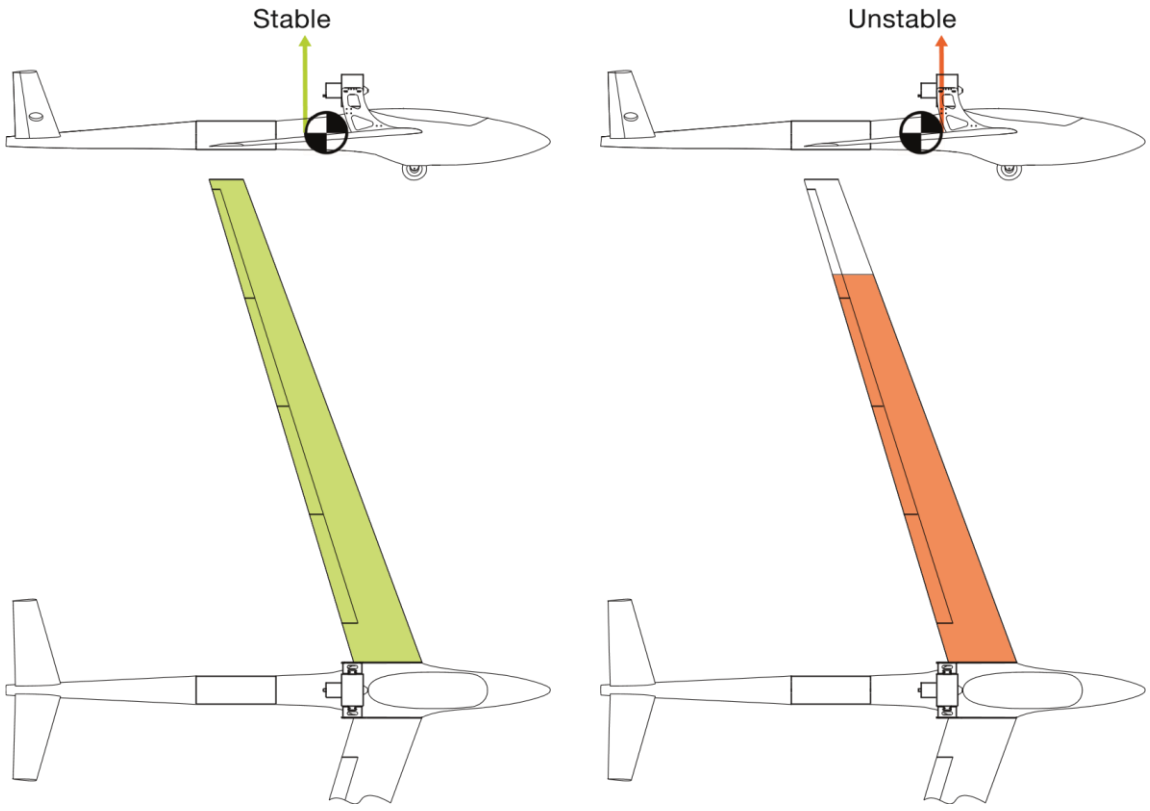

Figure 9 - Exemplification: Shift of neutral point due to wing tip stall.

Since the concerns of a disability to recover from a stalled flight state could not be ruled out conclusively, it was decided to implement a generous safety margin by raising the minimum allowed airspeed in the operational guidelines. Among others, this lead to high take-off speeds that were operationally critical due to the ground handling capabilities during taxi.

In order to assess the stall behaviour of the *T-FLEX* flight demonstrator, without testing the *T-FLEX* demonstrator itself due to the high risk involved, it was decided to build a subscale flight demonstrator with a take-off mass below 25 kg, for this allowed rather simple flight tests on RC-airfields. Due to the high risk involved the subscale demonstrator should rely on commercial-off-the-shelf (COTS) components wherever possible.

3.2 Demonstrator Design and Specifications

The design resembles the configuration of the *T-FLEX* demonstrator, while being scaled considering the scaling laws for dynamic demonstrators mainly developed by Wolowicz [2] and more currently described by Sobron[3], and practical consideration concerning the manufacturing possiblities at the Institute of Aircraft Design. A 3-side view is presented in the following Figure 10, more detailed technical data described in the Table 2.

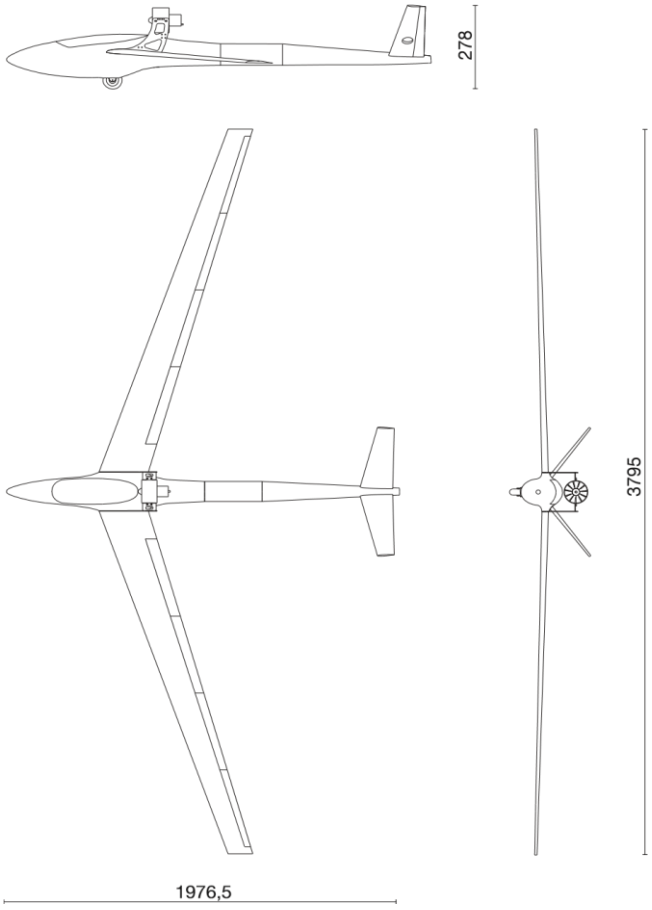

Figure 10 - 3-Side view of DeFStaR (dimensions in [mm]).

Table 2 - Characteristic specifications of the DeFStaR dynamic demonstrator.

Symbol	Value	Unit	Characteristic
n	0,53	–	Scaling factor
A_{wing}	0,723	m^2	Wing area
Λ_{LE}	20,00	deg	Leading edge sweep angle
Γ	0,00	deg	Dihedral angle
AR	19,92	-	Aspect ratio
λ	2,00	-	Taper ratio
c_{root}	0,250	m	Root chord length
MAC	0,198	m	Mean aerodynamic chord length
x_{COG-LE}	0,320	m	X-COG position from root leading edge
v_{stall}	13,00*	m/s	Stall speed
v_{max}	60,00*	m/s	Maximum speed
$MTOM$	11,00*	kg	Maximum take-off weight

*estimate

The aerodynamic properties on configuration level were assessed using a model incorporating wing and fuselage in the software *XFLR5*. In order to assure similar flow conditions, the pressure distribution of the profile *try6* was compared at the different Reynolds-Numbers at which *T-FLEX* demonstrator and the *DeFStaR* subscale demonstrator were expected to stall (see Figure 11) using the program *X-FOIL* and no substantial deviations found.

It needs to be pointed out clearly, that a forced transition at 5% chord-length was assumed. This was implemented using the same trip-band as used on the *T-FLEX* demonstrator making the assumption that a trip-band that is capable of enforcing a transition on the *T-FLEX* demonstrator is capable of enforcing a transition on the smaller *DeFStaR* subscale demonstrator. A different COTS trip-band typically used on RC-aircraft was considered but was rejected due to a deviation in shape (zig-zagged vs. straight) and dimensions both in terms of height and depth.

The electrical systems comprised of COTS components to implement the remote control functionality. A Pixhawk 4 running a PX-4 flight stack was incorporated to record in-flight data. The sensor package includes IMUs and gyroscopes as well a GPS and Air Data sensor. The aerodynamic angles were not measured directly. A similar setup was proven suitable already during comparable, earlier tests. Additionally, the electrical system incorporated a mixer, that allowed the modulation of a multi-sine signal on the control inputs of the ruddervators and the adjustment of the amplitude using a secondary remote control.

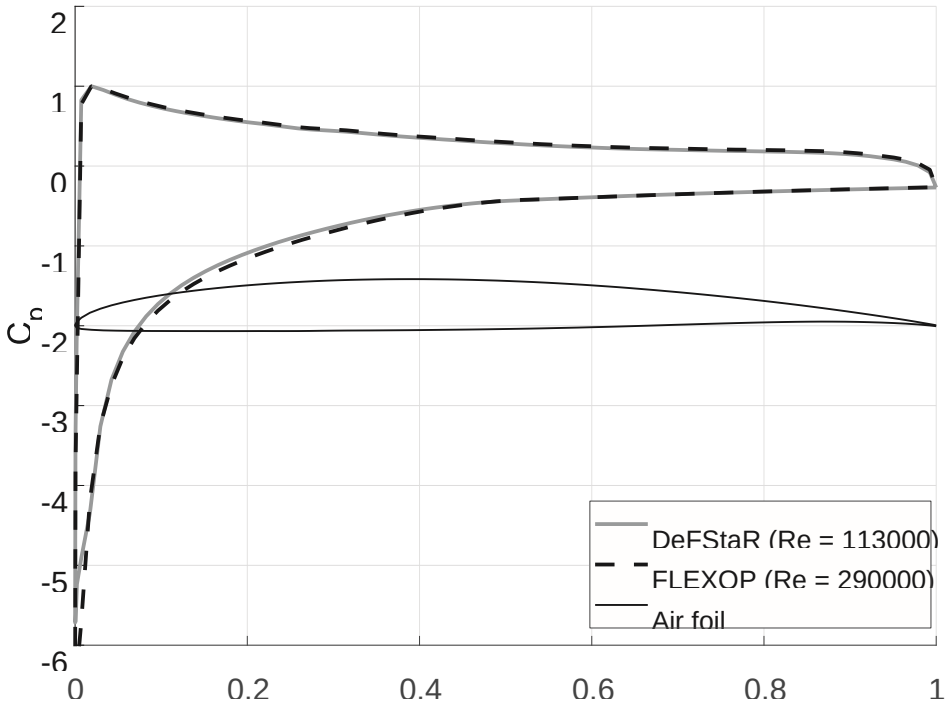

Figure 11- Cp-polars at 13° angle of attack.

3.3 Design Verification and Flight Testing

The subscale demonstrator was tested on ground and in flight to verify the targeted dynamic similitude (similitude of mass moments of inertia and aerodynamics), before the actual stall tests were conducted. The relevant details and results are outlined in the following sections.

3.3.1 Ground Testing

Next to ground tests assuring the airworthiness and systems checks, efforts concentrated on determining the mass moments of inertia by using a bifilar pendulum for adjustment to the values required by the methods of dynamic scaling. The frequency of the rotational oscillation was determined from video using the analysis software Tracker. The measurement yielded deviation of up to 13%, however, were not adjusted in order to keep the take-off mass low for the maiden flight. The adjustment was done later in-field with using the Steiner's Law.

3.3.2 Flight Testing

First, the flight tests conducted focused on determining the aerodynamic derivatives to verify the aerodynamic similitude using methods of system identification. Subsequently, the flight tests to assess the stall behavior were conducted.

Flight Tests for System Identification

The stall behaviour is greatly influenced by the pitching moment due to a change of angle of attack α, expressed by the aerodynamic derivative $C_{m\alpha}$. Therefore, flight experiments focused on determining the aerodynamic derivative $C_{m\alpha}$ by exciting the short period mode and identifying the parameters of a reduced, linearized, decoupled 2x2 state space model of the short period mode and subsequently determining the value for $C_{m\alpha}$. For exciting the short period mode, multi-sine inputs, that were modulated on the pilots inputs in the ruddervators, were used, since pulse- and doublet-inputs had been used for similar investigations and yielded unsatisfactory results and multi-sines have received wide recognition in recent publications [4]. Default inputs scaled to 1 were designed based on an estimation of expected

frequencies using the program *Athena Vortex Lattice 3.37*, the final amplitude was determined during flight tests by continually increasing the amplitude using the secondary transmitter connected to the mixer until the pilot stopped the increase. A total of 24 flight experiments were conducted on two test days.

Flight Tests for Stall Behaviour Assessment

For the stall tests, the wing was equipped with tufts on the upper side of the left that were filmed during the experiments by two action cams fixed to the dorsal engine mount, additionally the experiments were filmed from the ground commented by readings of the airspeed values received in the telemetry data. The procedure of stall testing was rather simple and straight forward: After climbing to an altitude deemed sufficient by the external pilot the throttle was reduced to zero causing the aircraft to decelerate while the elevator was deflected upwards in order to maintain altitude until the attitude could not be maintained any further. Two different flap deflections were tested: A landing configuration that featured a large deflection on the most inner flap and a take-off configuration that featured decreasing flap deflections on all four flaps one wing. Prior to the stall tests, the chosen flap configurations had been tuned based on the experiences collected during take-off and landing for the test flights for conducting experiments for system identification.

3.4 Presentation of the Results

In the following, the results of the flight tests are described.

3.4.1 Results of System Identification

Out of the 24 flight test experiments conducted, 12 proved to be suitable for the identification of parameters describing the short period mode. The parameter values identified showed relatively good fit, as is exemplified in the following Figure 12 showing the fit of the data of the second flight test day.

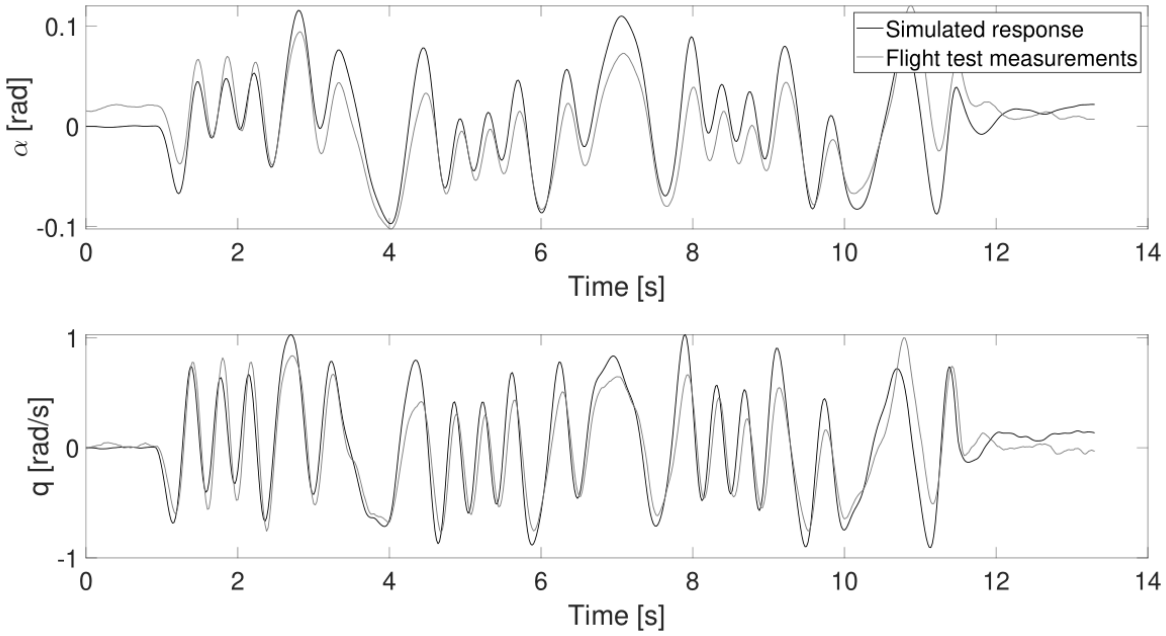

Figure 12 - Comparison of the simulated model response to day two flight test measurements.

During data evaluation it became apparent, that two different configurations in terms of center of gravity location were tested on the different testing days. The aerodynamic derivative $C_{m\alpha}$ was determined to an

average value of $C_{m\alpha} = -1.71$ on the first day, and to an average value of $C_{m\alpha} = -1.42$. This means, that the stall tests were conducted with the less stable configuration. Since the *DeFStaR* subscale flight demonstrator was not equipped with an airdata probe providing aerodynamic angles, it was not possible to determine the absolute values of the aerodynamic coefficient C_m. Therefore, the value at zero angle of attack $Cm0$ was determined with the model implemented in *XFLR5*. The resulting plot of the aerodynamic coefficient C_m over the angle of attack α is shown in Figure 13 below.

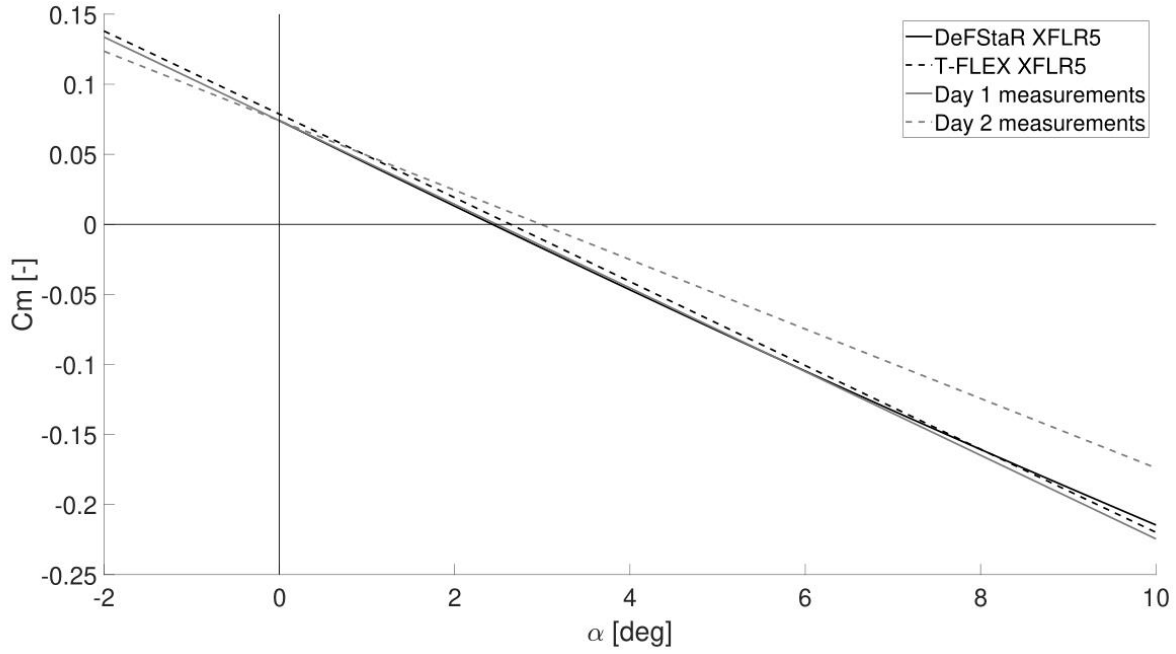

Figure 13 - Comparison of the Cmα polars from XFLR5 and flight test data.

As becomes apparent in Figure 13 above, all lines except the one labelled ”T-FLEX XFLR5” intersect at an angle of attack $\alpha = 0$ which is a consequence of accepting the same value for the aerodynamic coefficient C_{m0} from the *XFLR5* simulation labeled ”DeFStaR XFLR5”. The line labeled ”Day 1 measurements” coincides well with the lines belonging to the *XFLR5* simulations of the *DeFStaR* subscale and *T-FLEX* demonstrator, indicating a suitable application of scaling methods. The line resembling the results of the flight test experiments conducted on the second test day, labeled ”Day 2 measurements” evolves with the smallest inclination and thus the smallest value for the aerodynamic coefficient C_m at higher angles of attack α. It is therefore to be expected, that the stall behaviour described in the following is more pronounced on the *DeFStaR* subscale demonstrator than on the larger, more stable *T-FLEX* demonstrator.

3.4.2 Results of Stall Behaviour Assessment

The assessment of stall behaviour is done qualitatively using a selection of stall-tests that comprise all different behaviours witnessed while good video footage and comments are available. The video footage was postprocessed and overlaid in order to get a better understanding of the impressions evolving. It can be viewed under the following link:

https://youtu.be/ZE44NFiudh8

Generally speaking, three different kinds of behaviour can be observed: The departure over a wing/a flipping motion, a ”plunging” flight state in which the aircraft maintains attitude while losing altitude rapidly

and the departure over a wing followed by a short (flat) spin. The stall tests are summarized in the following Table 3.

Table 3 - Overview of selected stall tests and respective behaviour as visible in the video accessible under the following link: https://youtu.be/ZE44NFiudh8.

No.	Stall speed	Configuration	Stall start	Observed behaviour
3	12 m/s	Landing	Wing tip	
4	11 m/s	Landing	Wing root	Plunging flight
5	12 m/s	Landing	Wing tip	Departure over left wing
6	11 m/s	Landing	Wing tip	Plunging flight
7	11-13 m/s*	Take-off	Wing root	Departure over right wing
8	11-13 m/s*	Take-off	Wing tip	Departure over left wing with spin

* The comments in the video are very close to another.

The synchronization cannot be assured to that accuracy.

The *DeFStaR* subscale demonstrator stalled at airspeeds $V \approx 12\text{m/s}$. The characters of witnessed behaviours covered a large range: While the aircraft was comparably easy to handle in the ”plunging” flight phases in which the pilot even reported acceptable roll authority despite a wing that exhibited separated flow over large regions, the occasions in which the demonstrator departed over a wing was described as ”bad-tempered”. During test point 8, in which the demonstrator entered a spin. About 170m of altitude were lost before the aircraft was recovered into level flight.

All stall behaviours were countered by the external pilot and no damage was done the subscale demonstrator. The external pilot reported furthermore an unsteady flight behaviour before entering a stall.

By and large, it seemed that the ”Landing” configuration was more benign in terms of stall behaviour, which can be explained by an ”overloading” of the inner wing segment by increased flap deflection. It needs to be pointed out, however, that the beginning of the stall is not a clear indicator of the stall behaviour, since the the onset was at the wing root, both during test 4 and 7, but resulted in different behaviours (”plunging” flight during test 4, departure over right wing during test 7). This underlines the complexity of the processes and the difficulty of predicting the stall behaviour, even in a qualitative manner only.

3.5 Conclusion

The *DeFStaR* subscale demonstrator was designed as a dynamic model of the *T-FLEX* demonstrator, implemented and proved suitable after ground and flight testing. Stall tests were conducted, documented using primarily video cameras and evaluated qualitatively. The following conclusions can be drawn:

- During the take-off phases of the *DeFStaR* various flap settings were tested. The take-off distances changed significantly in between the different trials. It was therefore concluded, that flap settings should be revisited for the *T-FLEX* demonstrator as well.
- The behaviour during stall exhibited differed to large extent, from steady post-stall sinking flight to a spin. This points to a complex state of flow that is difficult to predict and hence supports the chosen approach using a subscale demonstrator.

- The loss of about 170 m of altitude between stall-onset and recovery in level flight during flight test 8 underlines the risk involved in stall testing, supporting the approach of using rather inexpensive COTS components.

4 Flight Test Reports

Multiple flight attempts were made since the first project flight in April, 2021. But with exceptionally bad weather this summer and technical issues while already in the airport, no flights took place in the period May-August.

For example, during flight preparations in July, a problem with the engine was discovered. It took the whole month to perform multiple tests with both engine units (spare and in-use), as well as to check the whole wiring. It was found that the control cable, going to the engine control unit, was broken. This meant that the engine sometimes would start going full-throttle and the pilot would not be able to control, neither shut the engine down. This was seen as hazardous risk and updates on the RXMUX software were made to eliminate the risk.

The two flights performed within this period so far are described below.

4.1 Flight Test 7

The goal of the FT7 were augmented mode and auto-throttle mode tests, familiarisation for the pilots and to perform trim points with different flap settings.

The mission was not completed in full. The flight had to be aborted after around 10 minutes due to a low voltage warning on one of the receivers. The problem was later identified and recorded (receiver logging lower voltage than the actual battery voltage).

Autothrottle functionality was tested during the flight.

Summary of the flight can be found in Table 4, followed by the corresponding graphs.

Table 4 - Summary of Flight Test 7.

Flight number:	**7**
Flight date:	21-Apr-2021 12:12:37
Take-off time:	12:17:23
Landing time:	12:27:27
Total flight time:	00:10:04
Total fuel used:	3.59kg
Original log filename:	41.mat
Analysis filename:	210421_1212_post.mat
Raw METAR:	EDMO 221950Z AUTO VRB01KT 9999 // NCD 04/M04 Q1022

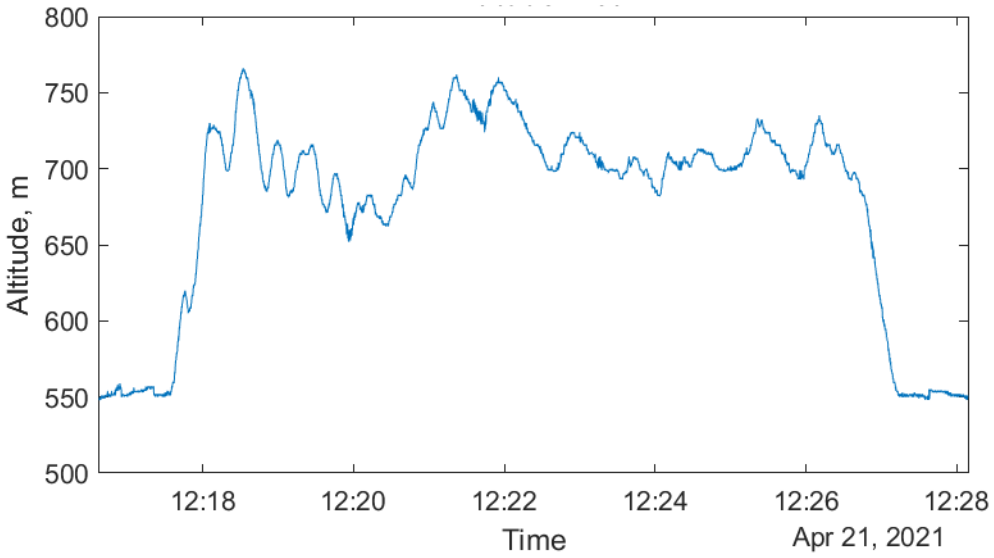

Figure 14 - Altitude plot, FT7.

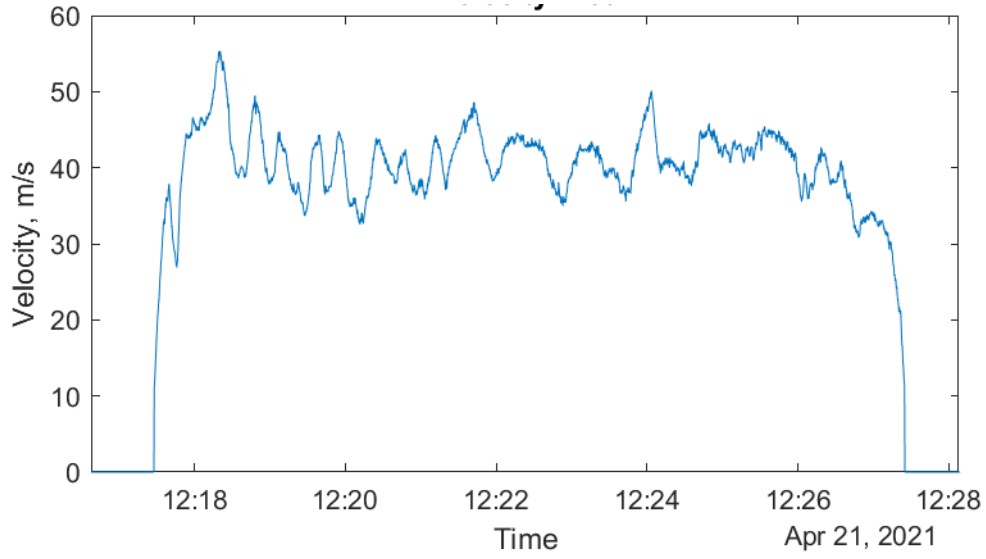

Figure 15 - Airspeed plot, FT7.

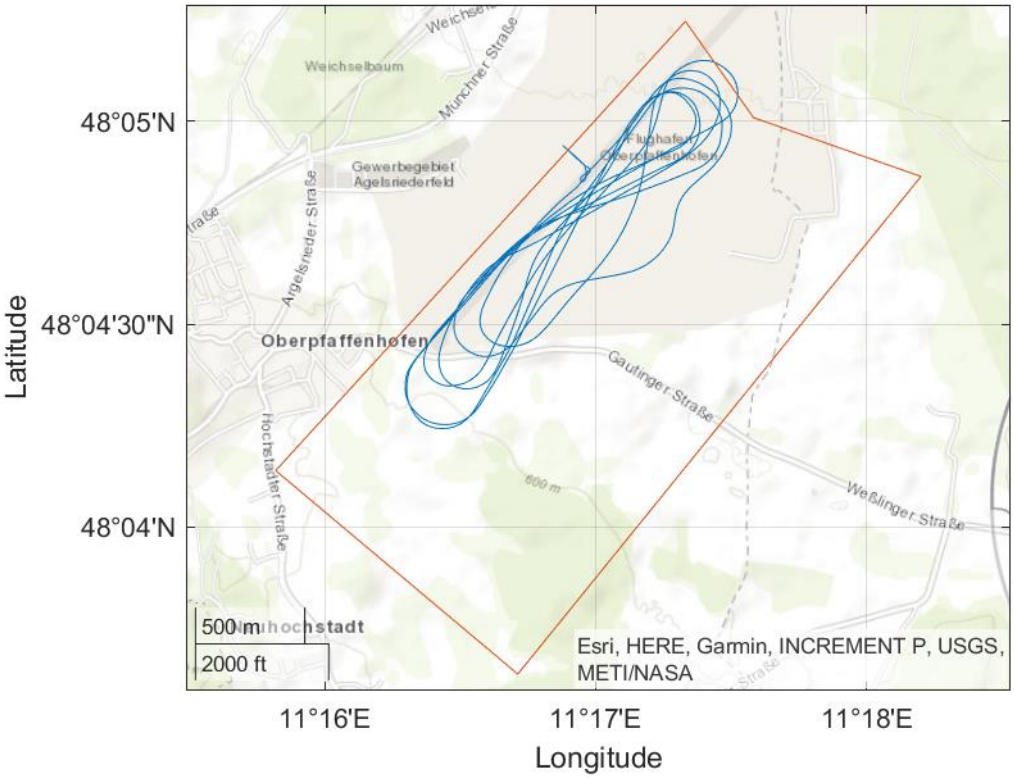

Figure 16 - Trajectory plot, FT7.

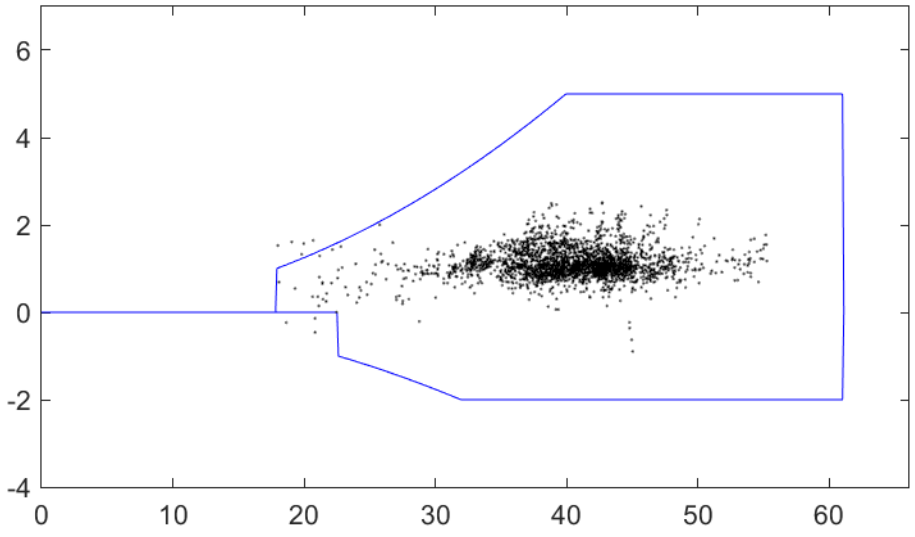

Figure 17 - Flight envelope, FT7 (x – airspeed, y – load factor).

The autothrottle segment was investigated. It was noted that the controller does not perform as expected. The engine control commands were very high frequency without allowing the engine to adapt (Figure 18). The effects can be seen in more detail in Figure 19. The module therefore required further adjustment.

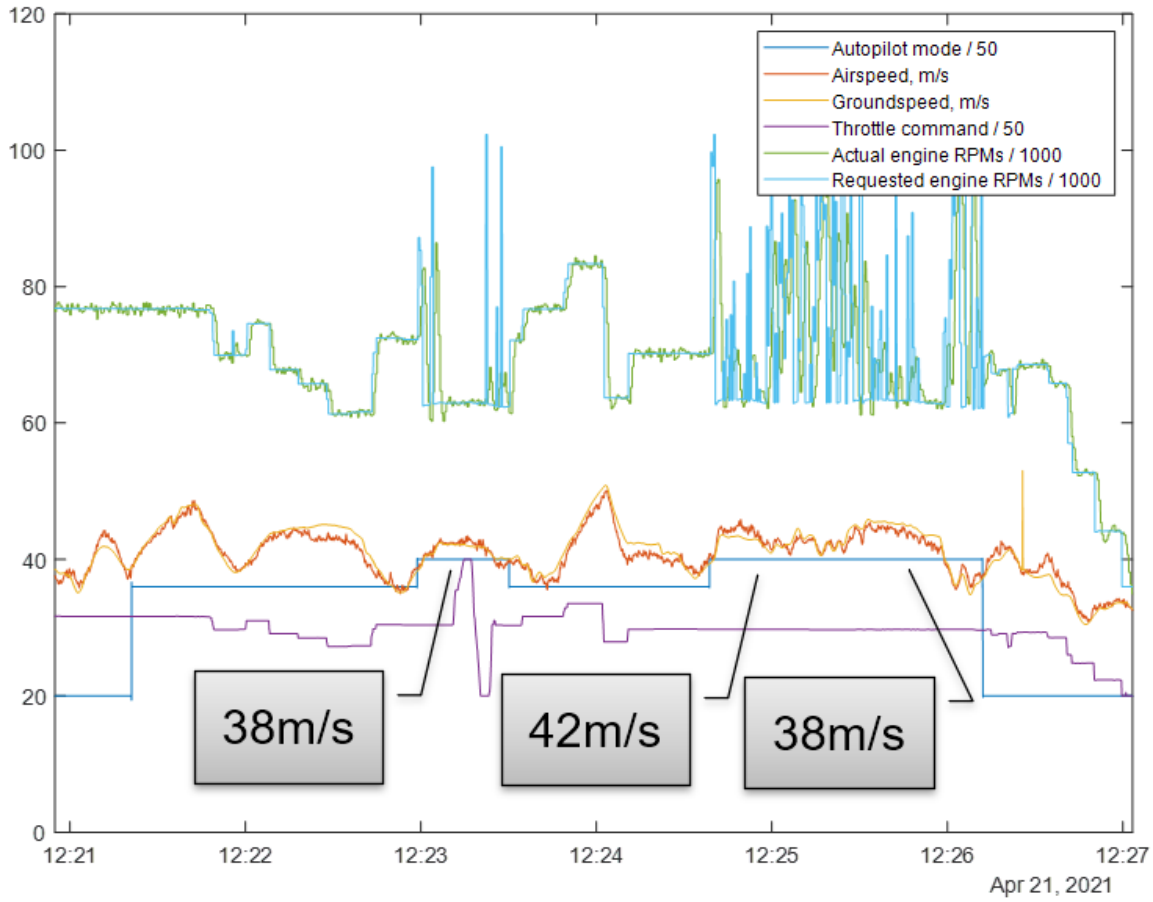

Figure 18 - Autothrottle testing during FT7. Two different speeds were used for the test. High frequency commands to the engine are visible.

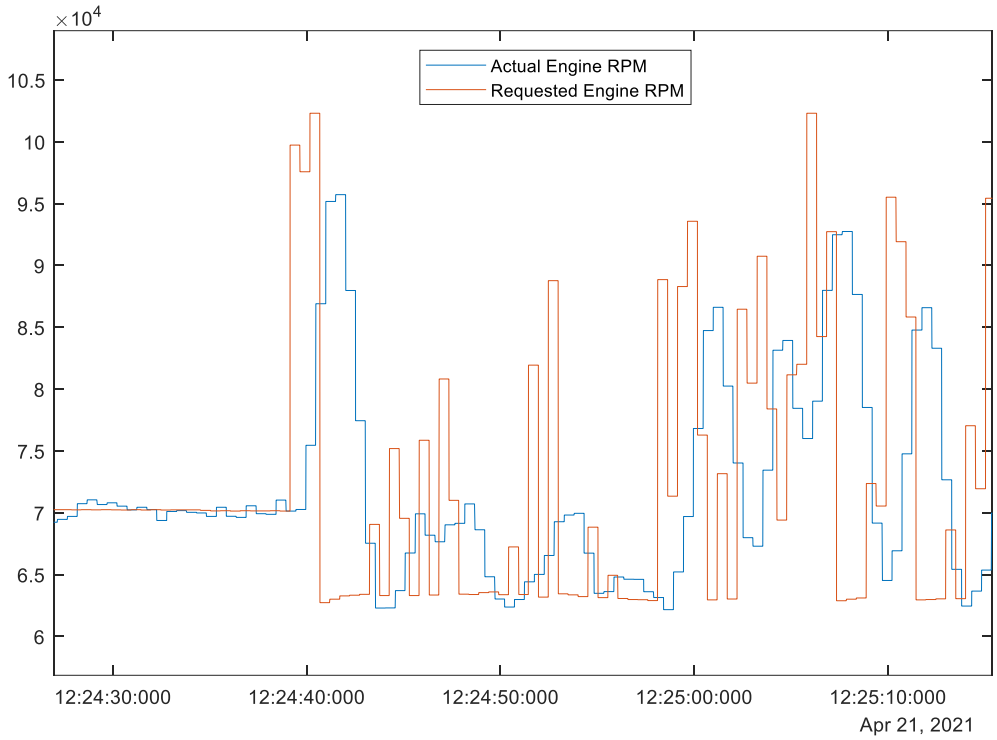

Figure 19 - The significant jumps in the RPM command sent by the autothrottle controller are clearly visible.

4.2 Flight Test 8

For the FT8, the goals were to perform the throttle injection tests and to get some familiarisation time for the pilots. The throttle injection tests were designed to get more idea about the engine model.

Four flight attempts were made before the Flight Test 8 happened. Most of the aborted flights were due to smaller issues that were only discovered during the start-up on-field. For example, a servo was accidentally broken during the start-up procedure, or there was an issue with the engine. However, the fourth attempt resulted in damage to the demonstrator. During the take-off, the demonstrator uncontrollably went to the side and hit a wooden post off the runway (Figure 20). Many small damages were recorded: tailwheel assembly completely broken (Figure 21), one damper of the main gear, two flap control linkages and the left airbrake servo were broken. The air-data probe was bent.

Figure 20 - The T-FLEX demonstrator after hitting the wooden pole during the FT8 take-off attempt.

Figure 21 - Screenshot of the tailwheel detaching from the fuselage during the FT8 attempt.

It took roughly a month to repair the aircraft and perform the actual FT8. Then the flight took place. The flight configuration inhibited many changes in comparison to the previous flight. All these configuration changes were based on the performance analysis, described in section 4.3. New flap settings were used, turbulators were removed, tailwheel control gains were reduced. 360deg camera was implemented, as well as the thrust measurement system was installed.

Unfortunately, the flight log was not captured properly. Due to a software bug and a human mistake, the log was accidentally deleted right after the flight, in preparation for the next one. All attempts to recover the log failed. Only video material, screen recordings of the GCS, the telemetry log (Figure 22) and the data from thrust measurement system (Figure 23 - Thrust Measurement System log during the FT8.) remained.

The flight however was seen as a success. New flap settings were approved, and the thrust measurement system was tested for the first time in-flight. Even though the thrust measurements need further correction of pitch and acceleration effects, the initial results look promising.

Table 5 - Summary of flight test 8

Flight number:	**8**
Flight date:	27-Oct-2021
Take-off time:	13:19:02
Landing time:	13:29:36
Total flight time:	10:30
Total fuel used:	-
Original log filename:	-
Analysis filename:	-
Raw METAR:	EDMO 271350Z 05008KT CAVOK 14/07 Q1024=

Another goal of the flight was to perform the throttle injection tests. As a preparation step, the augmented mode was engaged. An unexpected behaviour with flap was noticed. FLAP 2 and FLAP 3 were oscilating in an unpredictable manner, high in amplitude and frequency. The mode was switched off after a few seconds. Another trial was done on the next test leg, but same phenomena occurred.

It is not yet clear what caused the oscilation. Investigation is also more difficult due to not having the proper flight log.

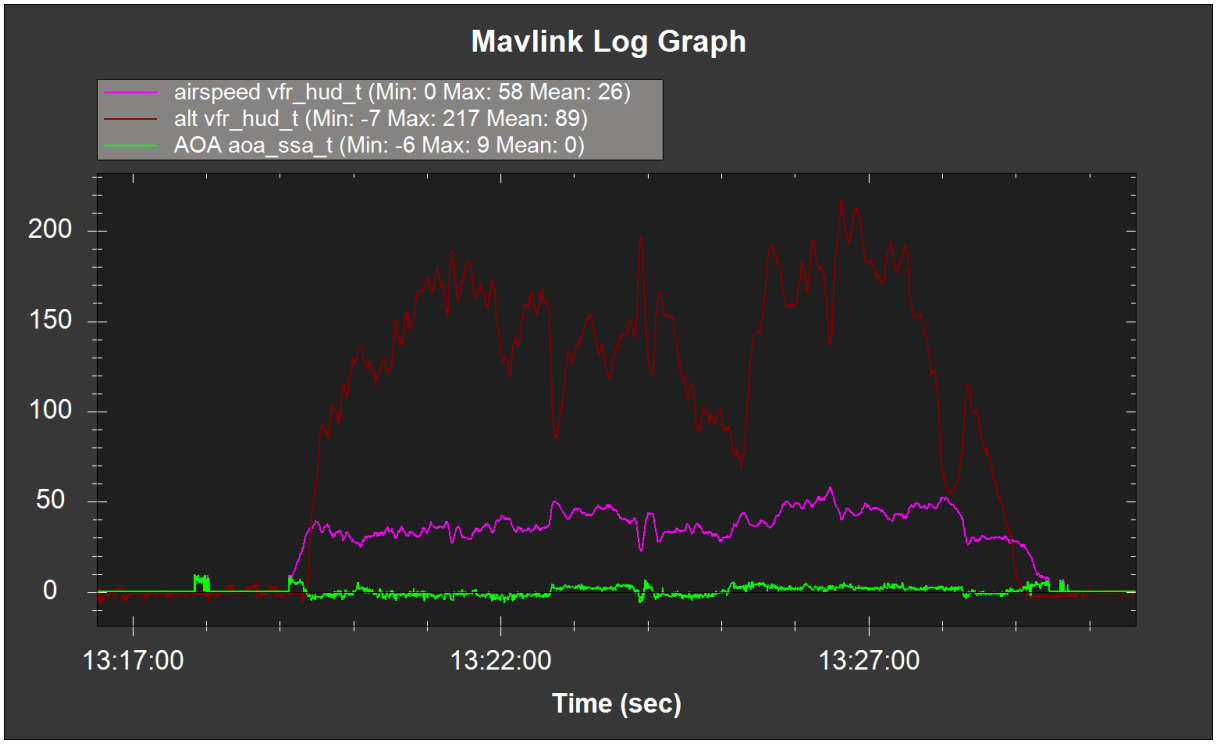

Figure 22 - FT8 flight log from telemetry data.

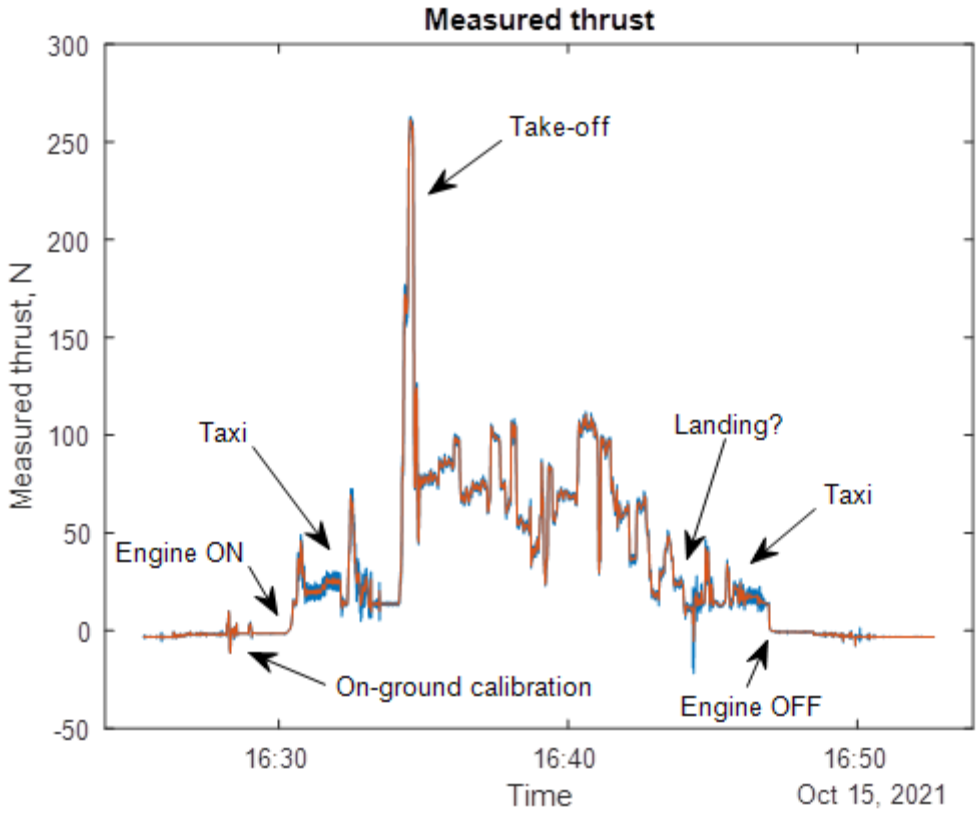

Figure 23 - Thrust Measurement System log during the FT8.

4.3 Flight Test 9

As it was impossible to reconstruct the log lost in FT8, the flight had to be repeated. The goal of the FT9 was to again test the stabilization mode of the autopilot and perform the throttle injections.

The flight was successfully performed. Multiple throttle injections were performed. Same unexpected behaviour of the autopilot was noticed with flaps starting to oscilate when the stabilization mode is switched on. The reason for the flap oscilation will be investigated further.

Table 6 - Summary of flight test 9.

Flight number:	**9**
Flight date:	**10-Nov-2021**
Take-off time:	**14:40:07**
Landing time:	**14:51:07**
Total flight time:	**00:11:00**
Total fuel used:	**4.15kg**
Original log filename:	**4.mat**
Analysis filename:	**211110_0154_post.mat**

The thrust measurement system was again tested and worked without any problems. The results of this flight will be used to publish a conference article about the design, development and testing fo the thrust measurement system [5].

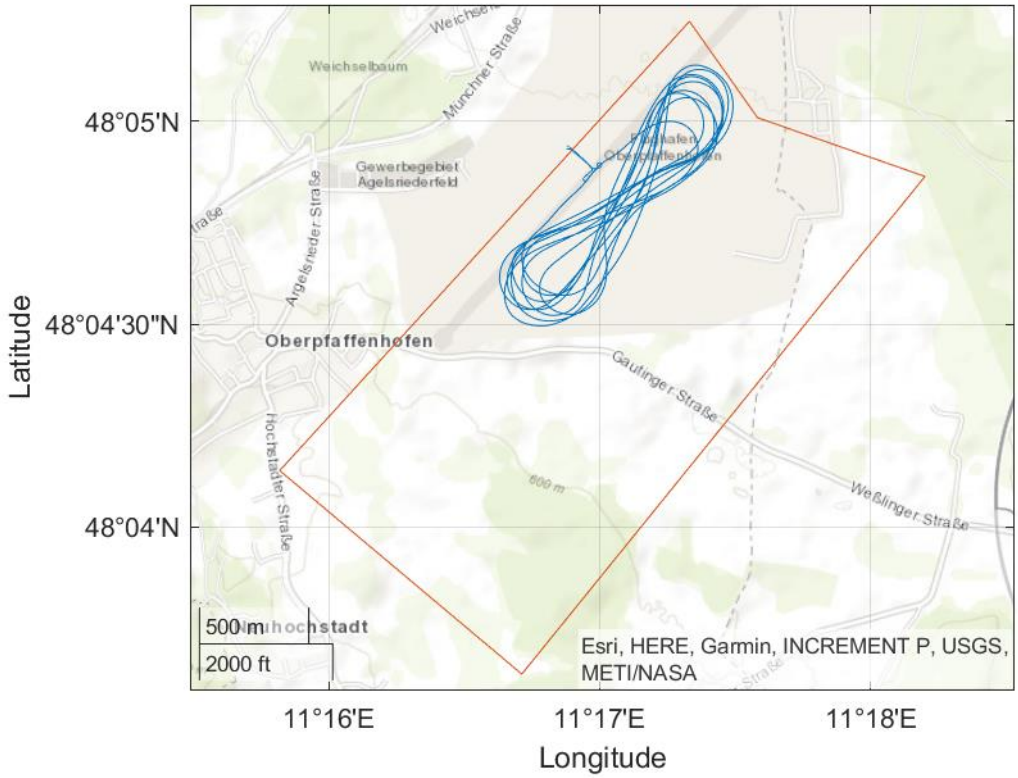

Figure 24 - Flight trajectory of the FT9

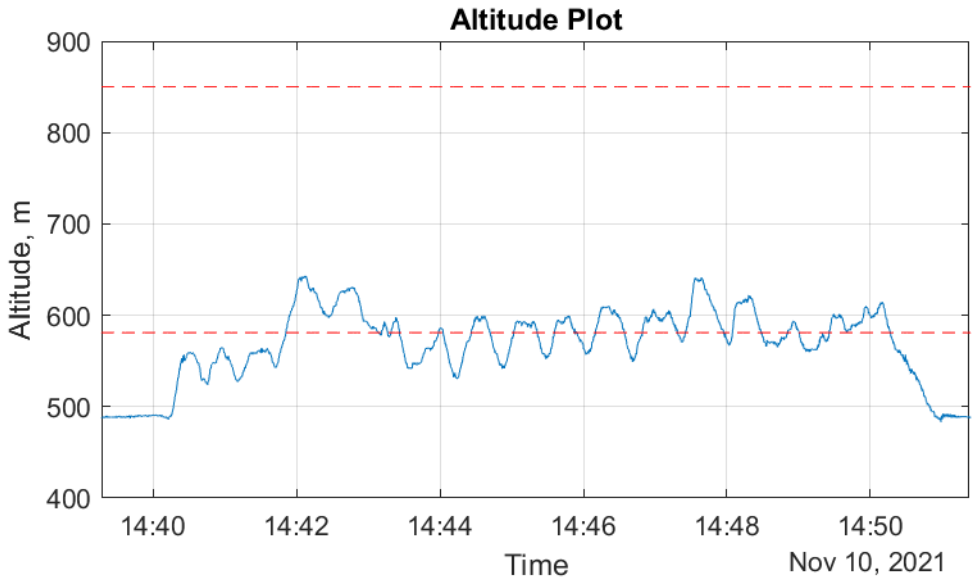

Figure 25 - Altitude plot fo the FT9.

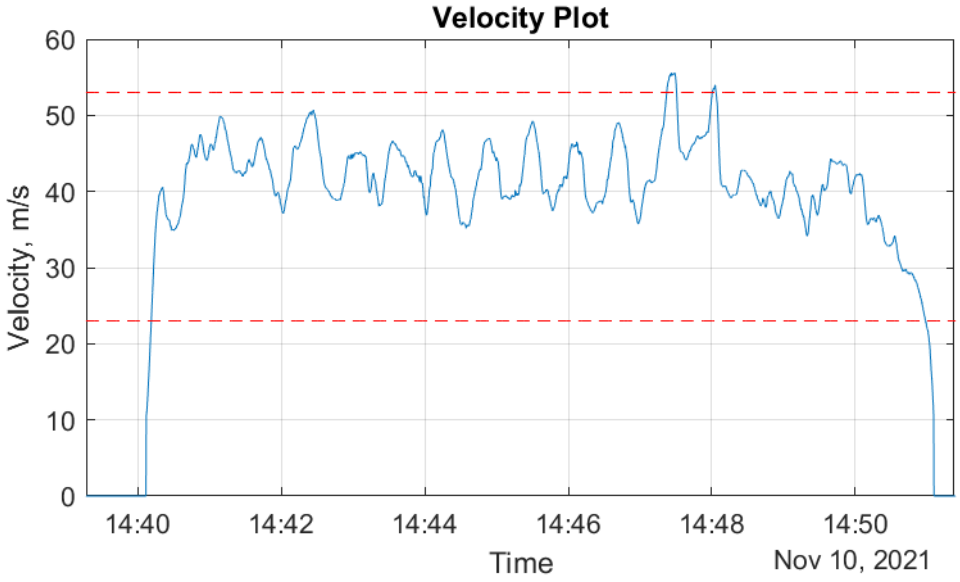

Figure 26 - Airspeed plot of the FT9. The throttle inputs are clearly visible.

5 T-FLEX Flight test analysis

5.1 Lift curve analysis

To check for consistency in between the previous flight test campaigns, analysis of the FT7 was done.

Lift curve was investigated for clean configuration. Steady-level flight points were extracted from FT7 and compared to steady-level flight points and steady turn points from FT5 (Figure 27). Furthermore, theoretical estimation of the lift curve was added.

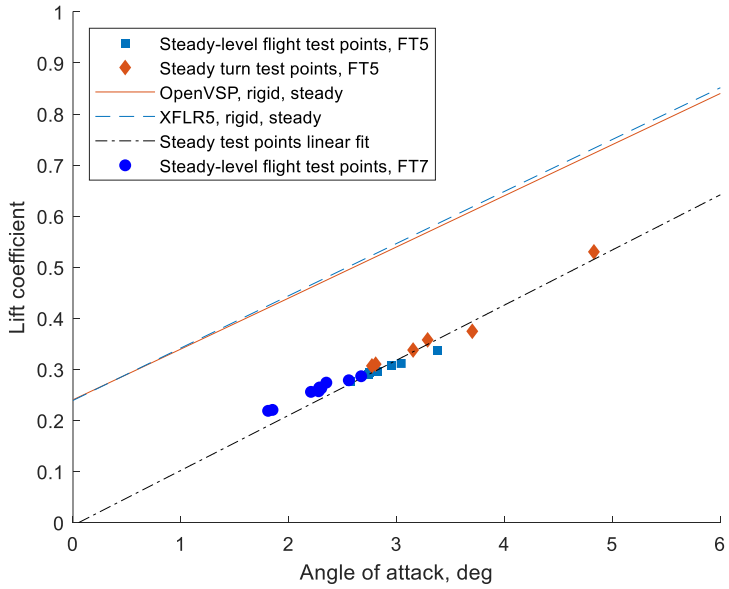

Figure 27 - Lift comparison (theoretical and in-flight data).

The following was noted:

- Lift curve as measured in-flight did not correspond to the theoretical estimations made by XFLR5 [6] and OpenVSP [7] software. An almost constant lift coefficient offset of around 0.2 can be observed which results in 35-45% lift loss in the 2-4deg angle of attack region.
- FT5 and FT7 data do align in the same trend.

The differences in between FT5 flight test data and theoretical estimations were already noticed before. However, initially it was assumed that maybe there are some errors in measurement of the angle of attack. After checking the alignment of the angle of attack probe, this suggestion was declined.

The reason for not achieving the estimated lift is being further investigated. Two potential cases are being checked:

- Loss of lift due to gaps in between the flaps and (section 5.3).
- Wing flow separation due to bad turbulator design (section 5.4).

Unsteady lift coefficient curves from pushover-pull-up manoeuvres from FT5 were also compared (Figure 28).

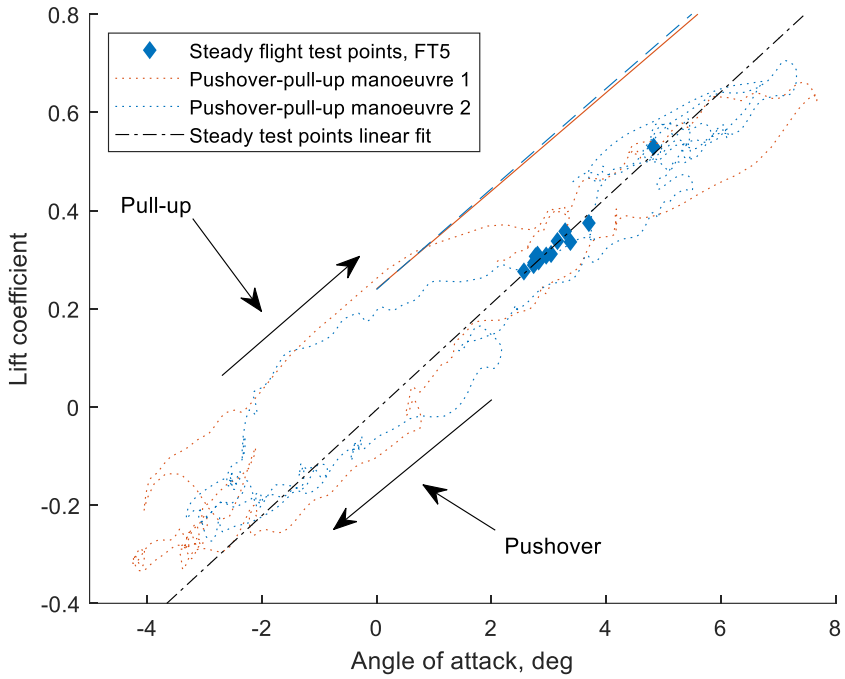

Figure 28 -Change of lift coefficient during pushover-pull-up manoeuvres.

It was noted that the lift coefficient values during the pull-up do match the theoretical predictions, while during pushover they fit in the same offset as the steady state manoeuvres. This could be an indication that the flow is indeed separated on a big part of the wing already at low angles of attack and it gets reattached during a pull-up.

Same loss of lift was noted for deflected flap case (take-off and landing configurations) as well.

5.2 Take-off data analysis

To better understand the bad take-off performance of the aircraft, detailed analysis of each take-off was done. Relevant data was plotted (Figure 29 is an example from FT2) and specific take-off run points extracted. These points were summarised in Table 7.

Figure 29 - Take-off data from Flight Test 7.

Table 7 - Take-off data summary. Values are averages from FT1, FT3, FT5, FT6, FT7. FT2 and FT4 were excluded due to high wind.

Nr	Description	Time, s	Distance, m	Airspeed, m/s	GPS Speed, m/s	Altitude (AGL), m	Throttle (command), %	Throttle (actual), %
1	Throttle up	-3.0	0.0	0.0	0.0	0	57	34
2	Start moving	0.0	0.3	0.0	0.5	0	100	83
3	Reach stall speed	4.4	43.0	18.0	16.5	0.8	100	100
4	Reach theoretical take-off speed	6.6	91.0	24.0	23.2	0.2	100	100
5	Take-off point (5m AGL)	10.7	198.2	33.9	31.9	5.3	100	100
6	Take-off finished (13m AGL)	12.8	267.8	36.7	35.1	13.4	100	100

What can be noted in the take-off data is that the lift-off airspeed, taken at 5m AGL is way higher than the design airspeed (34m/s vs 24m/s, or 42% higher). This might point to the same loss-of-lift problem as discussed in previous section.

5.3 Influence of flap gaps

It was contemplated that the gaps in between the flaps, which are not covered in the case of T-FLEX, might be the reason of pressure loss on the lower side of the wing. Such effect was noted by [8] (Figure 30).

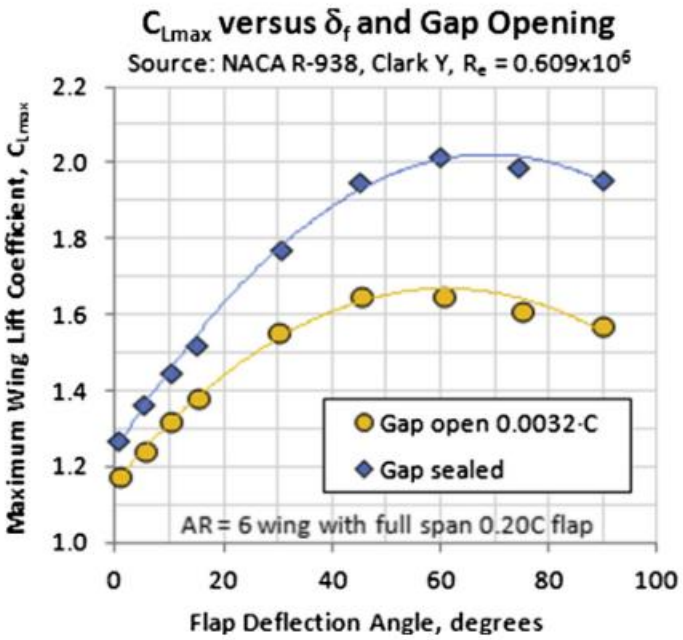

Figure 30 - The effect of gap on the magnitude of maximum lift coefficient [8].

From Figure 30 big amount of lift can be lost due to the untreated flap gaps. However, this effect is mostly present at big angles of attack and increases with increasing the flap deflection. The loss is also in a lower order of magnitude than we expect. Therefore, it was decided, that even though this effect could play a role to recover the lift for T-FLEX, it probably is not the main problem.

As a result, the flap gaps were covered with special tape on the lower side of the wing.

5.4 Turbulator analysis

The influence and design of the turbulators was checked.

From the available documentation of the turbulator design, the 0.22mm high, 5mm width 3M tape was chosen. This decision was made based on multiple sources, references in a presentation (Figure 31).

To confirm this, two methods were used again – an unreferenced Excel sheet from Lockheed Martin (was also used in the initial design) and a well referenced method of Braslow and Know [9]. Initially, the current design location was reproduced (x/c = 0.05) for three airspeeds (20, 30 and 60m/s). Then the location was shifted backwards, and the effect was investigated.

The resulting minimum thicknesses for the turbulator to be effective were at least double of the previous design (Table 8). Both methods agreed on this. Therefore, it was concluded that the initial design was not effective and most likely did not influence the flow as expected. As the maximum available turbulator size was 0.4mm, three different designs were suggested (changing the turbulator location), to meet the minimum thickness criterion.

In the end it was decided to only use the turbulator for the FLAP 4.

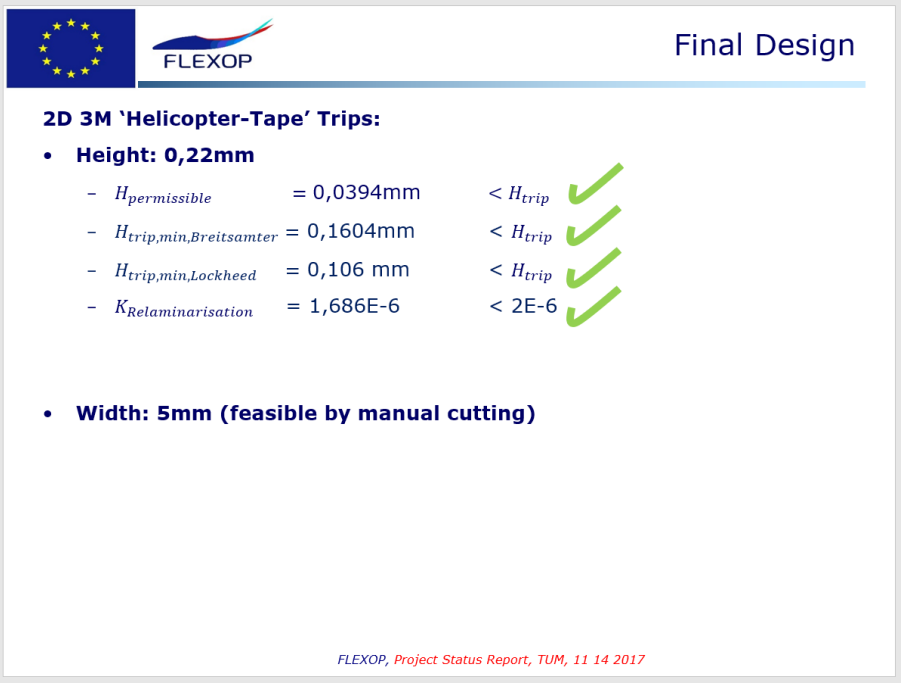

Figure 31 - Documentation of turbulator design process in FLEXOP project.

Table 8 - Comparison of minimum turbulator thickness. Current and 4 suggestion designs are presented. Note that the actual turbulator that was applied on the wing was 0.2mm - half of the recommended height.

			suggested trip, mm	
configuration	turbulator at x/c	velocity, m/s	Braslow and Knox [9]	Lockheed chart
current	0.05	20	0.48	0.46
	0.05	30	0.34	0.33
	0.05	60	0.19	0.20
suggestion 1	0.10	20	0.53	0.53
	0.10	30	0.37	0.39
	0.10	60	0.21	0.23
suggestion 2	0.15	20	0.56	0.58
	0.15	30	0.40	0.42
	0.15	60	0.23	0.25
suggestion 3	0.20	20	0.59	0.62
	0.20	30	0.42	0.45
	0.20	60	0.25	0.27
suggestion 4 (only FLAP 4)	0.20	20	0.59	0.62
	0.20	30	0.42	0.45
	0.20	60	0.25	0.27

Next it was investigated if the transition location could have a big effect on the lift curve. The 2D lift curve for the aerofoil with and without the turbulator was calculated. This was done with two methods: 2D aerofoil solver XFOIL and a CFD code TAU.

The following conclusions were made:

1. The influence of the turbulator is negligible with TAU code.

2. The change of the forced transition location does have an influence with XFOIL code. The difference in between the cases with and without the turbulator is in the order of $\Delta C_L = 0.05$.
3. XFOIL does calculate higher lift than the TAU code.
4. Inviscid solution predicts a way higher lift than either XFOIL or TAU code. The difference is in the order of magnitude of $\Delta C_L = 0.10 - 0.15$.

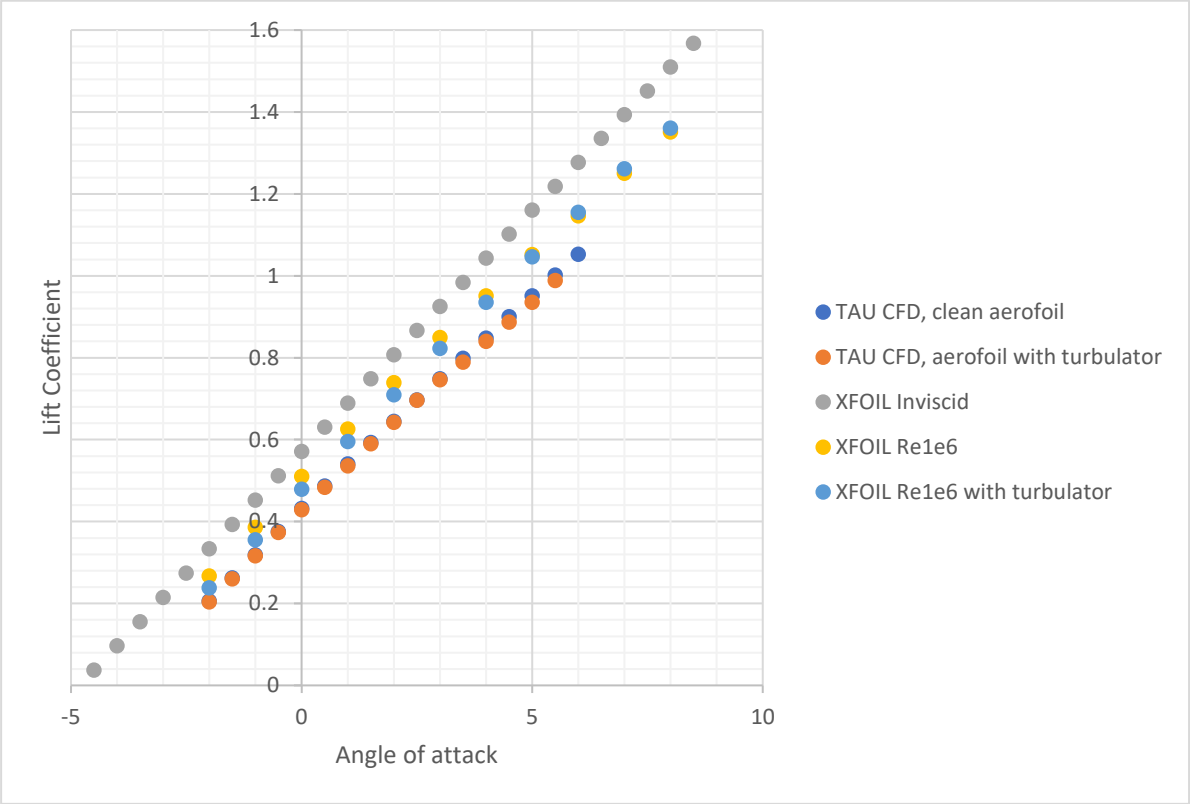

Figure 32- Comparison of coefficient of lift with and without the turbulator.

Initially it was thought that there is a significant portion of lift (around 40%) missing on the aircraft. This was based on comparing the available flight test data and the aerodynamic analysis done before. It was proposed that this effect might be due to the bad turbulator design or the unsealed flap gaps. After investigating both options it was concluded that neither of those two effects should amount to the required order of magnitude. But it was discovered that the inviscid solution, which was used for all the aerodynamic calculations in the project, has a significantly higher lift values than the viscous. It probably could be accounted to the viscous decambering effect. This could explain the discrepancies in between the modelling and flight tests.

For the future aerodynamic modelling, Reynolds number effects should be considered.

5.5 Flap setting analysis

Building on previous flight experience it was decided to revisit the flap settings designed for the take-off and landing phases.

Initial configuration had only one flap (the most innerboard) deflected- 10deg for take-off and 25deg for landing. These deflections theoretically were supposed to increase the lift by around $\Delta C_L = 0.13$ and $\Delta C_L = 0.27$ respectively. It was decided to look for different flap deflection configurations that would decrease the take-off run further.

For the analysis, the VSPAERO solver was used [7]. The solver is a non-viscous VLM based solver. It was clear that the absolute values of any coefficients would be different than in reality, but in this case, only the relative trends were of interest.

The design space was kept within the three innerboard flaps. This was due to the possible tip-stall with a swept wing if FLAP 4 would accidentally reach higher angles of attack. 9 configurations were investigated in total. The deflections and their performance (in terms of lift and moment coefficients) are presented in Table 9 (results are graphed in Figure 33 and Figure 34). Additionally, the effect of full thrust (for example during go-around) on moment coefficient was investigated (Figure 35).

Table 9 - Flap setting investigation for take-off and landing phases. The final configuration is marked with blue and grey colors.

Configuration	FLAP 1	FLAP 2	FLAP 3	FLAP 4	AoA	CL	CMy	Cmy with engine
0/0/0/0	0	0	0	0	0	0.22957	0.137	0.055
0/0/0/0	0	0	0	0	4	0.64348	0.007	-0.075
10/0/0/0	10	0	0	0	0	0.35152	0.185	0.103
10/0/0/0	10	0	0	0	4	0.76442	0.050	-0.032
25/0/0/0	25	0	0	0	0	0.49921	0.248	0.166
25/0/0/0	25	0	0	0	4	0.90723	0.111	0.029
10/10/0/0	10	10	0	0	0	0.47078	0.149	0.066
10/10/0/0	10	10	0	0	4	0.88257	0.010	-0.072
10/10/5/0	10	10	5	0	0	0.51786	0.108	0.026
10/10/5/0	10	10	5	0	4	0.92904	-0.030	-0.112
15/10/5/0	15	10	5	0	0	0.57307	0.131	0.049
15/10/5/0	15	10	5	0	4	0.98496	-0.016	-0.098
20/15/5/0	20	15	5	0	0	0.67694	0.136	0.054
20/15/5/0	20	15	5	0	4	1.0826	0.000	-0.082
25/10/5/0	25	10	5	0	0	0.66537	0.172	0.090
25/10/5/0	25	10	5	0	4	1.07183	0.031	-0.051
30/15/5/0	30	15	5	0	0	0.75546	0.17066	0.089
30/15/5/0	30	15	5	0	4	1.15266	0.02235	-0.060

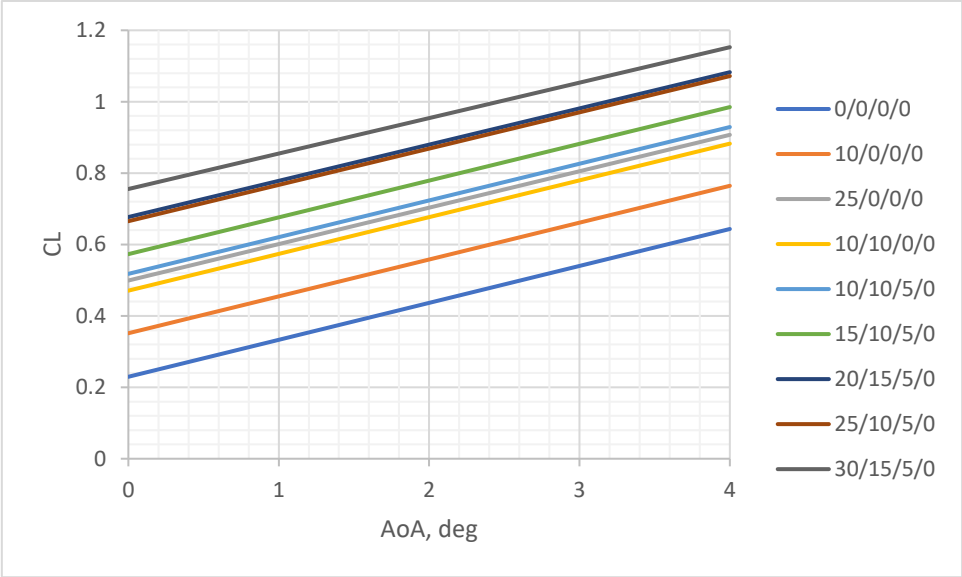

Figure 33 - Lift coefficient for different flap settings.

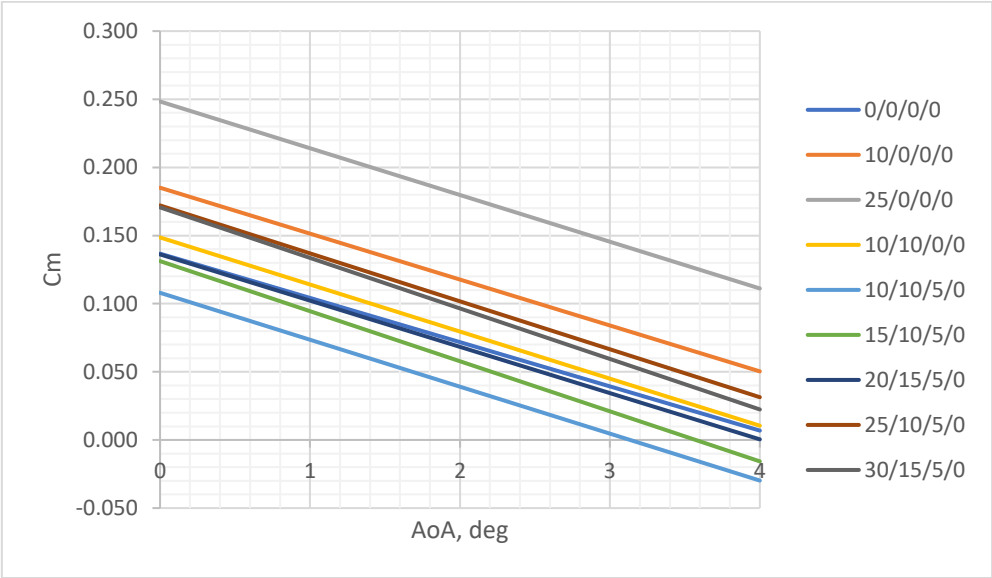

Figure 34 - Moment coefficient for different flap settings.

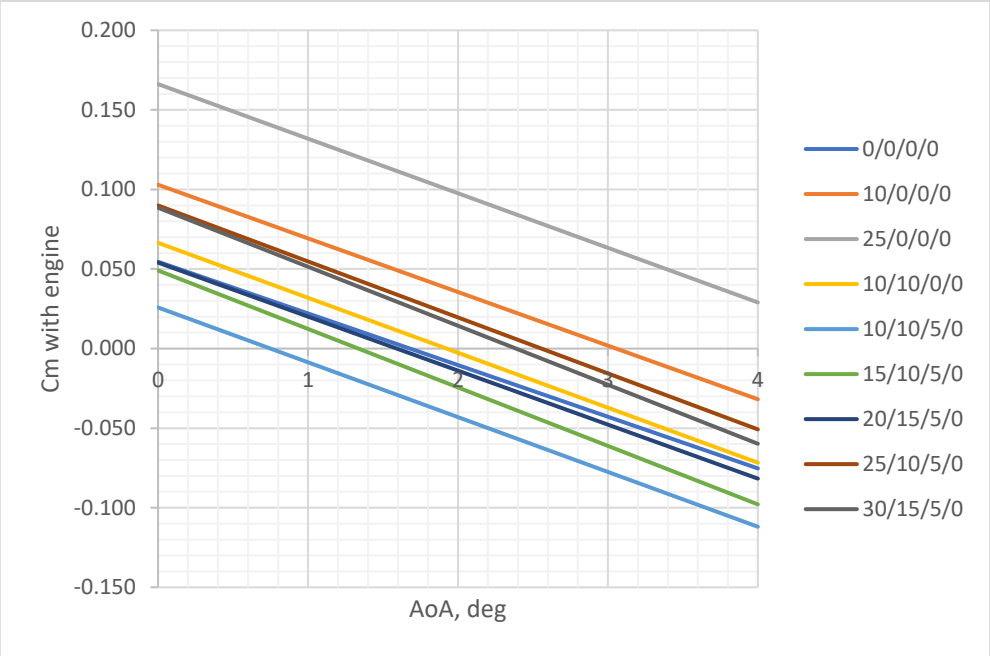

Figure 35 - Moment coefficient for different flap settings with the full thrust effect included.

After analysing all the flap configurations, it was noted that the single flap deflection produced significant pitching moment. This was also noted during flight, where the trim had to be significantly different from the cruise configuration (marked with 0/0/0/0).

After analysing all the options, two final configurations were selected: 20/15/5/0 for take-off and 30/15/5/0 fro landing.

The take-off configuration (20/15/5/0) was supposed to (theoretically) provide almost double the lift of previous take-off configuration while also decreasing the resulting moment coefficient. This is due to the deflection of the FLAPS 2 and 3, which, due to sweep, balance the aircraft.

For landing configuration (30/15/5/0), even further increase in lift was made. Also, a configuration with higher pitch moment was chosen to balance the higher angle of attack for landing. This also helps in a situation of a go-around, when full thrust is applied, and aircraft tries to pitch down.

5.6 Thrust measurement system data analysis

The system has been tested in-flight. Up to date, two test flights were done with the system. Results from one of them will are presented.

Thrust was logged throughout the whole flight, including the engine start-up phase. Measured and modelled thrust is compared in Figure 36. For this comparison, thrust model based on engine revolutions, Mach number and altitude, developed during a different project was used. Even though the two methods agree well at very low thrust values, an almost constant offset of 10N is seen during the rest of the flight. One reason for this might be that the engine model does not take the ambient temperature into account.

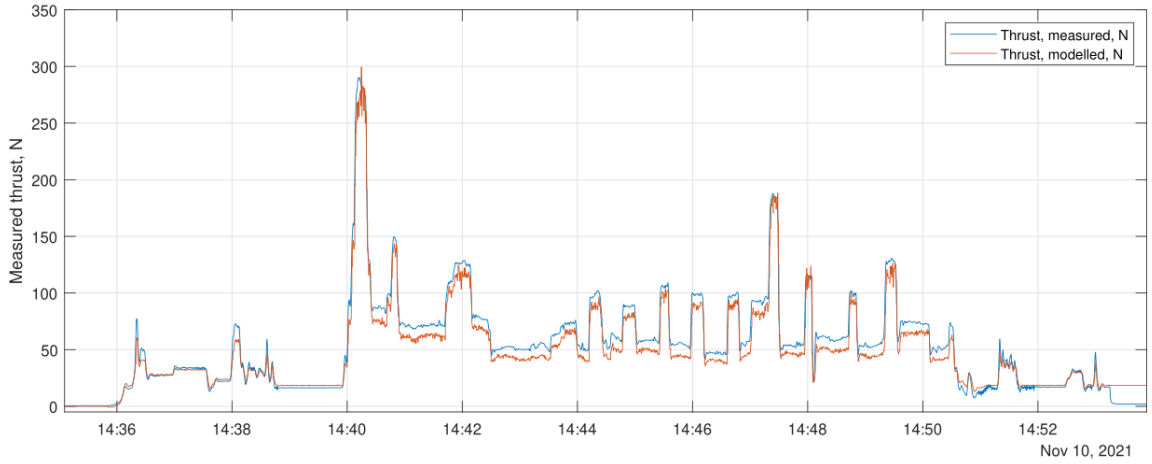

Figure 36 - Thrust measured during flight. For comparison, thrust modeled with respect to engine revolutions, Mach number and altitude is added.

An extract of two throttle step inputs is shown in Figure 37. The lower sampling frequency of the engine revolutions, in comparison to the rest of the flight variables, can be noted. However, the thrust measurement system does follow changes in the engine spool speed well.

After reviewing the measured thrust, some trends of the system could not yet be explained. During the moments of high yaw rates, the system tend to have jumps in logged thrust, as can be seen in Figure 37. Even though the yaw rate is accounted for when changing the coordinate system of accelerations from the aircraft to the engine mount assembly, there still seems to be an unexplained component that influences the final measurement. Another unexplained increase in measured thrust is also marked. Both of these trends seem to appear only in highly unsteady motion. Further investigation for the cause will follow.

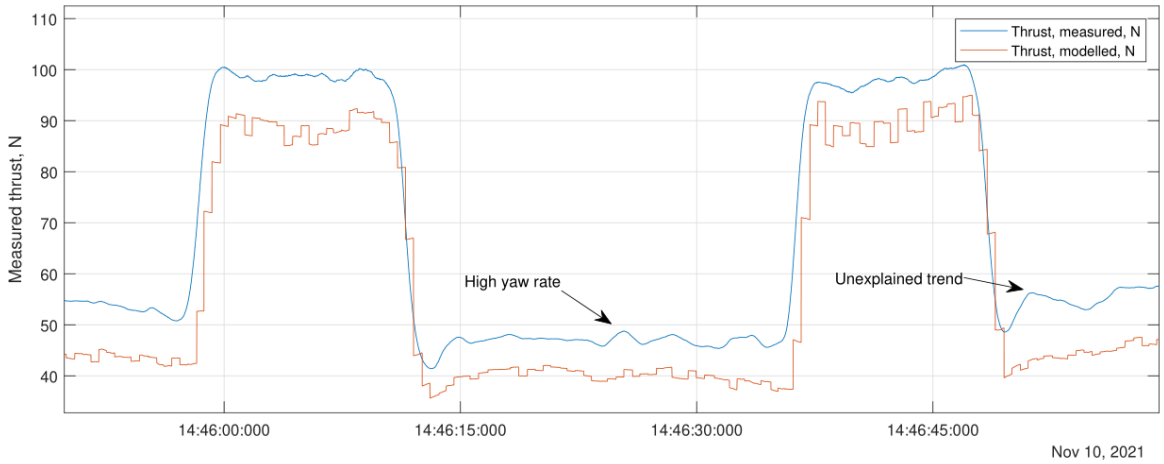

Figure 37 - Measured thrust during a throttle step input.

6 Conclusion and outlook

Deliverable 3.2 – Flight Test Report Phase #1 describes the taxi tests, sub-scale stall tests, T-FLEX flight tests and aerodynamic analysis performed within years 2020 and 2021. Main outcomes from the report are:

- The faulty initial design of the landing gear required big improvements for sustainable flight testing.
- Flight test data and further aerodynamic analysis revealed that the aircraft generates significantly less lift than initially predicted.
- Revised flap settings for take-off and landing configurations significantly improved the take-off and landing performance.

Up to date, only two flights were made in phase 1. The main objectives of the phase (autopilot functionality check and aerodynamic model creation) are not yet completed. Therefore, further flights are needed.

It is currently expected that at least 5 more flights are needed. However, with the improvements on the aircraft this year, it is planned to finish phase 1 at early spring 2022, the latest.

7 Bibliography

[1] B. Scheufele, “Development , Flight-Testing and Evaluation of a Subscale Dynamic Demonstrator to Re- produce the Stall Behavior of a Large Swept Wing Research UAV,” Technical University of Munich, 2021.

[2] C. H. Wolowicz, J. S. . J. Brown, W. P. Gilbert, J. S. . J. Brown, and W. P. Gilbert, “Similitude requirements and scaling relationships as applied to model testing.” 1979.

[3] A. Sobron, “On Subscale Flight Testing: Applications in Aircraft Conceptual Design,” Linköping University, 2018.

[4] E. A. Morelli, “Flight Test Maneuvers for Efficient Aerodynamic Modeling,” *J. Aircr.*, vol. 49, no. 6, pp. 1857–1867, 2012.

[5] J. Bartasevicius, P. Alexandre, T. Fleig, A. Metzner, and M. Hornung, “Design and testing of an in-flight thrust measurement system for a pylon-mounted miniature jet engine,” 2022, pp. 1–16.

[6] A. Deperrois, “Guidelines for XFLR5: Analysis of foils and wings operating at low Reynolds numbers,” 2013.

[7] B. Litherland and K. Rieth, “VSP Aircraft Analysis User Manual Modeling and Analyzing Aircraft Designs Using Parametric Geometry Tools and Vortex Lattice Software 1 National Aeronautics and Space Administration,” 2014.

[8] Snorri Gudmundsson, *General Aviation Aircraft Design*. 2016.

[9] A. L. Braslow and E. C. Knox, “Simplified method for determination of critical height of distributed roughness particles for boundary-layer transition at Mach numbers from 0 to 5,” p. 19, 1958.